

# Untangling Knots Through Curve Repulsion



DRAFT

Candidate Number: (Redacted)  
Honour School of Mathematics (Part C)  
University of Oxford  
Trinity Term 2023

# Untangling Knots Through Curve Repulsion

## Abstract

Curves are one of the fundamental objects in geometry and engineering, yet most analysis of curves often disregard their physical characteristics such as their spatial volume or uncrossability. One common situation that such physical characteristics become significant is when one attempts to untangle a knot. An approach to achieve this is to assign an “energy” to a curve such that this energy would increase when two points on “different sides” of a curve are closer, then one continuously deforms the curve to reduce this energy, the expectation being that the curve that achieves minimal energy must be the “unknot”. This dissertation explores numerical methods of achieving this.

## Contents

<b>1</b>	<b>Introduction</b>	<b>2</b>
<b>2</b>	<b>Gradient Flow Equation</b>	<b>3</b>
2.1	Motivation of Gradient Flow Equation . . . . .	3
2.2	Gradient of Functional . . . . .	5
2.2.1	Gradient on Integer Sobolev Spaces . . . . .	5
2.3	Derivative Operators for Curves . . . . .	7
<b>3</b>	<b>Finite Difference Method</b>	<b>8</b>
3.1	Motivating Example: Heat Equation . . . . .	8
3.1.1	First-Order Finite Difference Operator . . . . .	8
3.1.2	Second-Order Finite Difference Operator . . . . .	9
3.2	Euler Schemes for Heat Equation . . . . .	9
<b>4</b>	<b>Tangent-Point Energy</b>	<b>10</b>
<b>5</b>	<b>Unknotting Curves via Gradient Flow Equation</b>	<b>14</b>
5.1	Discretisation for Numerical Computation . . . . .	15
5.1.1	Discretisation of Curve . . . . .	15
5.1.2	Discretisation of Tangent-Point Energy . . . . .	15
5.1.3	Derivative Operators Discretised Curve . . . . .	18
5.1.4	Finite Difference Scheme of Curve Untangling Process . . . . .	19
5.2	Example: $L^2$ Explicit Euler Scheme . . . . .	19
5.2.1	Constraint Energy . . . . .	21
5.2.2	Time Complexity . . . . .	22
5.2.3	Discussion of Implicit $L^2$ Euler . . . . .	23
5.3	Example: Euler Scheme in $H^{-1}$ and $H^1$ . . . . .	23

<b>6 Conclusion, Outlook, and Potential Alternative Approach</b>	<b>27</b>
6.1 Possible Variations to Curve Untangling Process . . . . .	28
6.1.1 Varying Time Step . . . . .	28
6.1.2 Varying the Sample Points . . . . .	29
6.1.3 Discussion of Fractional Sobolev Space . . . . .	29
6.2 An Alternative Approach via Approximation Theory . . . . .	29
6.2.1 Curves in $\mathbb{S}$ . . . . .	30
6.2.2 Curves in $\mathbb{L}$ . . . . .	32
6.2.3 Sample Points and Time Complexity . . . . .	33
6.3 Potential Extension: Ribbon-like Objects . . . . .	35
<b>Appendices</b>	<b>39</b>
<b>A Definitions of Important Inner Product Spaces</b>	<b>39</b>
A.1 $L^2$ Space . . . . .	39
A.2 $H^k$ Space . . . . .	39
<b>B Gradient Operator in Sobolev Spaces</b>	<b>40</b>
<b>C Tangent-Point Energy Quadrature: Other Homeomorphism Classes</b>	<b>41</b>
C.1 Curves in $\mathbb{L}$ . . . . .	42
C.2 Curves in $\overline{\mathbb{L}}$ . . . . .	42
<b>D Exact <math>\ell^2</math> Gradient of <math>E_\beta^\alpha</math></b>	<b>43</b>

# 1 Introduction

Shape optimisation is an important idea in engineering, relevant in anywhere from aircraft designs to packaging ramen noodles. One of the simplest and most fundamental shapes to consider is a curve. While simple in concept, they prove to be quite difficult to analyse in practice with realistic physics. Even in absence of other objects, one must consider resilience to bending, stretching, and especially, impenetrability against itself. With these physical factors in mind, untangling a curve (Figure 1.1) becomes a very complicated process, especially in a computer simulation. This dissertation explores numerical methods to achieve this.

The main idea is to *assign energy that penalises “physical entanglement”*. Given a parameterised curve  $\gamma : M \rightarrow \mathbb{R}^3$  ( $M$  being the domain of the parameter, often an interval), one defines some *curve energy*  $\mathcal{E}$  of the form:

$$\mathcal{E}(\gamma) := \iint_{M^2} k(\gamma_x, \gamma_y) d\gamma_x d\gamma_y \quad (1.1)$$

where  $k \geq 0$  is the *curve energy kernel* such that  $k \rightarrow +\infty$  as  $|\gamma_1 - \gamma_2| \rightarrow 0^+$  where  $\gamma_1$  and  $\gamma_2$  are the two points “nearly-crossing”.

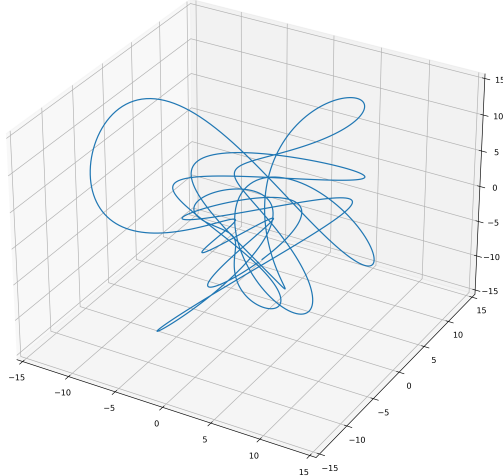


Figure 1.1: A tangled curve in  $\mathbb{R}^3$

A naïve choice of  $k$  satisfying this condition is  $k_S(\gamma_x, \gamma_y) := \frac{1}{|\gamma_x - \gamma_y|}$ . However, it turns out that  $k_S \sim O\left(\frac{1}{|\gamma_x - \gamma_y|}\right)$  as  $|\gamma_x - \gamma_y| \rightarrow 0$ , meaning the  $\mathcal{E}$  diverges all continuous curves  $\gamma$  of nonzero measure (consider neighbouring points).

A more analytically sensible choice of  $k$  would be the tangent-point kernel introduced in a paper by Buck and Orloff[4] and later generalised by Yu, Schumacher, and Crane[12].

The next part of the idea is to *reduce  $\mathcal{E}$  by continuously deforming the curve* based on a descent method until it reaches a stationary curve, at which, we expect it to be the “unknot” of the original curve. Note that by construction of  $\mathcal{E}$ , if the curve is to self-intersect,  $\mathcal{E}$  increases, and the descent method encourages the curve to repel, preventing the self-intersection.

## 2 Gradient Flow Equation

Since we pose the problem as continuous reduction of some functional, we need an applicable framework. In our case, **gradient flow equation** seems to be appropriate.

### 2.1 Motivation of Gradient Flow Equation

For minimising a differentiable function  $f : E \subset \mathbb{R}^n \rightarrow \mathbb{R}$ , there is a well-known method called **steepest descent method** (SDM)[2].

$$\mathbf{x}^{k+1} = \mathbf{x}^k - \alpha_k \nabla f(\mathbf{x}^k) \quad (2.1)$$

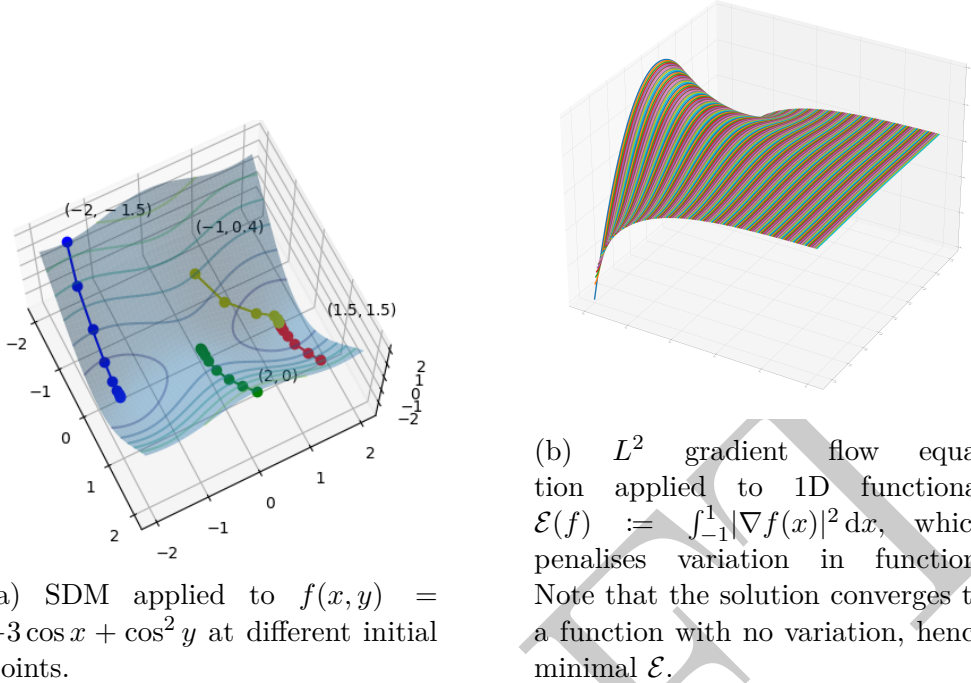


Figure 2.1: Gradient flow can be understood as a analogue of steepest descent to functionals.

Starting from the initial input point  $\mathbf{x}^0$ , at each iteration, input points  $\{\mathbf{x}^k\}$  move in the direction of “steepest” decrease, with specified step size  $\alpha_k > 0$ , reducing the value at evaluation of  $f$ . Note that in general, this method is not guaranteed to find the minimiser (Figure 2.1(a)). On the other hand, convergence is guaranteed under certain assumptions, for example, convexity and  $L$ -smoothness<sup>1</sup> with a certain choice of  $\alpha_k$ .

Analogously, differential equation describing the reduction process of a functional  $F : \mathcal{X} \rightarrow \mathbb{R}$  (where  $\mathcal{X}$  is an inner product function space) can be motivated. Starting from (2.1), replacing  $\mathbf{x}^k$  by  $f_k$  and  $\nabla f(\mathbf{x}^k)$  by  $\text{grad}_{\mathcal{X}} F(f_k)$ ,

$$f_{k+1} = f_k - \alpha_k \text{grad}_{\mathcal{X}} F(f_k) \quad (2.2)$$

Now think of  $f_k$  as “snapshots” at certain time  $t = t_k$ . Without loss of generality, let  $\alpha_k \equiv 1$ .<sup>2</sup> Dividing (2.2) by time step  $\Delta t := t_{k+1} - t_k$ , and taking the limit as  $\Delta t \rightarrow 0$ , we acquire the **gradient flow equation**[12].

$$\frac{\partial f}{\partial t} = - \text{grad}_{\mathcal{X}} F(f) \quad (2.3)$$

where index  $k$  transforms to “time” variable  $t$ .

---

<sup>1</sup> $|\nabla f(\mathbf{x}) - \nabla f(\mathbf{y})| \leq L |\mathbf{x} - \mathbf{y}|$  for some constant  $L > 0$

<sup>2</sup>This is justified by taking a different time scale; essentially nondimensionalisation. Also  $\alpha_k \sim O(1)$  as  $k \rightarrow \infty$  (eg.  $\alpha = L^{-1}$  for  $L$ -smooth optimisation) is in fact a realistic choice.

Note that grad of a functional is not defined yet. This depends on the inner product function space  $\mathcal{X}$  (eg.  $L^2$ ,  $H^1$ , ...) of interest.

## 2.2 Gradient of Functional

In order to understand the gradient of a functional, it helps to recall the gradient of a function. Gradient of a function  $f : \mathbb{R}^n \rightarrow \mathbb{R}$  characterises the first-order variation in a certain direction, that is,

$$\forall \mathbf{x}, \mathbf{y} \in \mathbb{R}^n \quad \nabla f(\mathbf{x}) \cdot \mathbf{y} = \frac{\partial}{\partial \epsilon} f(\mathbf{x} + \epsilon \mathbf{y})|_{\epsilon=0} \quad (2.4)$$

While this is not a conventional definition of function gradient, it is an equivalent definition.

One could analogously motivate the definition of functional gradient.

**Definition** (Functional Gradient). For a functional  $F : \mathcal{X} \rightarrow \mathbb{R}$ , define *functional gradient*  $\text{grad}_{\mathcal{X}} F(f)$  as:

$$\forall f, g \in \mathcal{X} \quad \langle \text{grad}_{\mathcal{X}} F(f), g \rangle_{\mathcal{X}} = \left. \frac{\partial}{\partial \epsilon} F(f + \epsilon g) \right|_{\epsilon=0} \quad (2.5)$$

where  $\langle \cdot, \cdot \rangle_{\mathcal{X}}$  is the inner product defined over the inner product function space  $\mathcal{X}$ .

Common inner product spaces include  $L^2$ ,  $H^1$ , which are introduced in Appendix A.

*Remark.* By assuming time-independence of  $f$  in the gradient flow equation (2.3), we get a stationary state equation  $\text{grad}_{\mathcal{X}} F(f) = 0$ , which implies  $\frac{\partial}{\partial \epsilon} F(f + \epsilon g)|_{\epsilon=0} = 0$  for all  $g \in \mathcal{X}$ . This shows that the stationary state of the gradient flow equation is precisely the solution to the Euler-Lagrange equation.

### 2.2.1 Gradient on Integer Sobolev Spaces

Assume  $\Omega$  is a boundary-free domain. Given  $L^2(\Omega) = H^0(\Omega)$  gradient ( $\Omega$  will be omitted when unambiguous), one could express Sobolev gradients of other orders. For functional  $F$ , write  $h := \text{grad}_{L^2} F$  for gradient of  $F$  in  $L^2$ , that is, by definition

$$\left. \frac{\partial}{\partial \epsilon} F(f + \epsilon g) \right|_{\epsilon=0} = \langle h, g \rangle_{L^2} =: \mathcal{P} \quad (2.6)$$

By lemma B.1 and lemma B.2 on boundary-free domain  $\Omega$ ,<sup>3</sup>

$$\begin{aligned} \mathcal{P} &= \langle \Delta \Delta^{-1} h, g \rangle_{L^2} \\ &= \langle -\nabla \Delta^{-1} h, \nabla g \rangle_{L^2} \\ &= \langle -\Delta^{-1} h, g \rangle_{H^1} \end{aligned}$$

So one could spot that

$$\text{grad}_{H^1} F = -\Delta^{-1} h \quad (2.7)$$

---

<sup>3</sup>Integration by parts to “shift” operators to other function.

*Remark.* However, there is a subtlety here. Because inverting a Laplacian requires additional information (often about the boundary, even though we assume it was a boundary-free domain),  $\Delta^{-1}$  can be problematic. One could resolve this by regularising  $\Delta^{-1}$  to  $(\Delta + c \text{Id})^{-1}$  where  $c \neq 0$  is a constant and  $\text{Id}$  is the identity operator. One justifies this replacement by noting the fact that  $H^1$  gradient is only defined up to addition of null space of the Laplacian<sup>4</sup>, and addition of  $c \text{Id}$  can make the operator invertible.

Similarly, one could acquire gradient in  $H^2$  by

$$\begin{aligned}\mathcal{P} &= \langle \Delta^{-1}h, \Delta g \rangle_{L^2} \\ &= \langle \Delta(\Delta^{-2}h), \Delta g \rangle_{L^2} \\ &= \langle \Delta^{-2}h, g \rangle_{H^2}\end{aligned}$$

Hence,

$$\text{grad}_{H^2} F = \Delta^{-2}h \quad (2.8)$$

One could extend by considering dual space[12] and define gradient in  $H^{-1}$ ,

$$\begin{aligned}\mathcal{P} &= \langle h, \Delta \Delta^{-1}g \rangle_{L^2} \\ &= \langle -\nabla h, \nabla(\Delta^{-1}g) \rangle_{L^2} \\ &= \langle -\Delta h, g \rangle_{H^{-1}}\end{aligned}$$

So,

$$\text{grad}_{H^{-1}} F = -\Delta h \quad (2.9)$$

*Remark.* From (2.7), (2.8), and (2.9), one may deduce that choosing the right Sobolev space for a functional may make the gradient flow equation much easier to solve.

**Example** (Dirichlet Energy). For example, given functional  $\mathcal{E}(f) := \int_{\Omega} |\nabla f(\mathbf{x})|^2 dV$  over an open set  $\Omega \subset \mathbb{R}^n$ , one can explicitly deduce  $L^2$  gradient from definition (2.5):

$$\begin{aligned}\langle \text{grad}_{L^2} \mathcal{E}(f), g \rangle_{L^2} &= \frac{\partial}{\partial \epsilon} \mathcal{E}(f + \epsilon g) \Big|_{\epsilon=0} \\ &= \frac{\partial}{\partial \epsilon} \int_{\Omega} (\nabla f + \epsilon \nabla g) \cdot (\nabla f + \epsilon \nabla g) dV \Big|_{\epsilon=0} \\ &= \int_{\Omega} \nabla f \cdot \nabla g dV \\ &\stackrel{\text{IBP}}{=} \underbrace{\oint_{\partial\Omega} g \frac{\partial f}{\partial n} dS}_{\text{Boundary Term}} - \int_{\Omega} g \Delta f dV \\ &= \underbrace{\oint_{\partial\Omega} g \frac{\partial f}{\partial n} dS}_{\text{Boundary Term}} + \langle -\Delta f, g \rangle_{L^2}\end{aligned}$$

---

<sup>4</sup>“Harmonic functions”

Assuming natural boundary condition  $\frac{\partial f}{\partial n} = 0$ , or restricting our interest to periodic functions such that there is no boundary, we may set the boundary term to zero. We can then read off  $L^2$  gradient to be  $\text{grad}_{L^2} \mathcal{E}(f) = h = -\Delta f$ . The gradient flow equation turns out to be the heat equation:

$$\frac{\partial f}{\partial t} = \Delta f \quad (2.10)$$

(Refer to Figure 2.1(b) for the case  $\Omega = (-1, 1)$ .) However, note that one could “reduce the order” or the RHS by considering the gradient flow in  $H^1$ . Observe from (2.7) that  $\text{grad}_{H^1} \mathcal{E}(f) = \text{Id}_\Omega f$ , where  $\text{Id}_\Omega$  is the identity operator. Solving  $H^1$  gradient flow equation

$$\frac{\partial f}{\partial t} = -f \quad (2.11)$$

is much easier as it boils down to solving an ordinary differential equation, which the solution decays (or rather converges) exponentially fast.

On the other hand, what if one reduces the order too much by taking  $H^2$ ? Since  $\text{grad}_{H^2} \mathcal{E}(f) = -\Delta^{-1} f$ , the  $H^2$  gradient flow equation becomes:

$$\frac{\partial f}{\partial t} = \Delta^{-1} f \quad (2.12)$$

This is solved by solving a Poisson’s equation  $\Delta g = f$  for  $g$ , then  $g = \frac{\partial f}{\partial t}$ , which is less practical.

## 2.3 Derivative Operators for Curves

For application of functional gradients on curves  $\gamma : M \rightarrow \mathbb{R}^3$ , the following derivative operators replace the traditional derivative operators,

**Definition** (First Derivative Operator “Curve Gradient”). Define first derivative operator[12]  $\tilde{\nabla}_\gamma$  in a way that for  $u(\gamma(\cdot)) : M \rightarrow \mathbb{R}$ ,

$$\tilde{\nabla}_\gamma u(\gamma(s)) = \frac{du(\gamma(s))}{|d\gamma|} \frac{d\gamma}{|d\gamma|} = \frac{du(\gamma(s))}{|d\gamma|} \underbrace{\mathbf{T}(s)}_{\text{Unit tangent at } s} \quad (2.13)$$

This encapsulates the tangential derivative with the actual direction of the tangent vector.

Similarly, for Laplacian,

**Definition** (Second Derivative Laplacian Operator “Curve Laplacian”). Define second derivative operator  $\tilde{\Delta}_\gamma$  in a way that for  $u(\gamma(\cdot)) : M \rightarrow \mathbb{R}$ ,

$$\tilde{\Delta}_\gamma u(\gamma(s)) = \tilde{\nabla}_\gamma^T \tilde{\nabla}_\gamma u(\gamma(s)) \quad (2.14)$$

### 3 Finite Difference Method

One of the simplest method to solve a differential equation is the **finite difference method**.[10]

#### 3.1 Motivating Example: Heat Equation

Suppose one needs to solve the heat equation  $\frac{\partial u}{\partial t} = \frac{\partial^2 u}{\partial x^2}$  for  $u = u(x, t)$  over  $[-L, L] \times [0, T_f]$  with initial data  $u(x, 0) = u_0(x)$  and Neumann boundary condition  $u'(-L) = u'(L) = 0$ .

One could discretise the problem by constructing a mesh; taking equispaced points on the spatial domain  $[-L, L]$  and the time domain  $[0, T_f]$ .

$$\begin{aligned} X_i &= -L + i(\Delta X) && \text{for } i = 0, 1, \dots, N \\ T_j &= j(\Delta T) && \text{for } j = 0, 1, \dots, M \end{aligned}$$

where  $N, M$  are the resolution of respective domains, and  $\Delta X := \frac{2L}{N}$  and  $\Delta T := \frac{T_f}{M}$ .

Now the idea is to approximate the initial boundary value problem by the following algebraic (difference) equations.

$$\mathcal{D}_t U_i^j = \mathcal{D}_x^+ \mathcal{D}_x^- U_i^j \quad (3.1)$$

$$U_i^0 = u(X_i) \quad (3.2)$$

$$U_0^j - U_{-1}^j = 0 \quad (3.3)$$

$$U_{N+1}^j - U_N^j = 0 \quad (3.4)$$

for  $i = 0, 1, \dots, N$  and  $j = 0, 1, \dots, M$ , where  $\mathcal{D}_z$  is a finite difference operator that approximates a derivative in  $z$  variable ( $t$  for time,  $x$  for spatial variable). Note that “virtual points”  $X_{-1}$  and  $X_{N+1}$  are added for discretised Neumann boundary condition (3.3) and (3.4). One interprets  $U_i^j$  as an approximation of  $u(X_i, T_j)$ .

##### 3.1.1 First-Order Finite Difference Operator

For utilising finite difference method for PDEs, one must choose an operator  $\mathcal{D}_z$  to approximate the derivative with respect to variable  $z$ .

Consider the **forward difference operator** to get an approximation of  $f'(z)$  at  $z = Z_i$ :

$$\mathcal{D}_z^+ f(Z_i) = \frac{f(Z_{i+1}) - f(Z_i)}{\Delta Z} = f'(Z_i) + \underbrace{O(\Delta Z)}_{\text{Consistency Error}} \quad (3.5)$$

Consider the **backward difference operator**, another approximation of  $f'(z)$  at  $z = Z_i$ :

$$\mathcal{D}_z^- f(Z_i) = \frac{f(Z_i) - f(Z_{i-1})}{\Delta Z} = f'(Z_i) + \underbrace{O(\Delta Z)}_{\text{Consistency Error}} \quad (3.6)$$

One can combine forward difference and backward difference to formulate the **central difference operator**, again for approximation of  $f'(z)$  at  $z = Z_i$ :

$$\mathcal{D}_z^{\circ} f(Z_i) = \frac{f(Z_{i+1}) - f(Z_{i-1})}{2\Delta Z} = f'(Z_i) + \underbrace{O((\Delta Z)^2)}_{\text{Consistency Error}} \quad (3.7)$$

Note that one could write  $\mathcal{D}_z^{\circ} f(Z_i) = \frac{1}{2}(D_z^+ + D_z^-) f(Z_i)$

While central difference operator may seem like the best choice in terms of consistency error, different choice of operators may result in much easier problem to solve albeit at the cost of increased consistency error.

### 3.1.2 Second-Order Finite Difference Operator

For PDEs involving second derivatives (such as the Laplace's equation), one must also be able to approximate the second derivatives with respect to variable  $z$ . A sensible choice is to use both the forward difference operator and the backward difference operator, known as the **second divided difference operator**:

$$D_z^+ D_z^- f(Z_i) = \frac{f(Z_{i+1}) - 2f(Z_i) + f(Z_{i-1})}{(\Delta Z)^2} = f''(Z_i) + \underbrace{O((\Delta Z)^2)}_{\text{Consistency Error}} \quad (3.8)$$

One can easily check that  $D_z^+ D_z^- = D_z^- D_z^+$ .

## 3.2 Euler Schemes for Heat Equation

Different choices for the first-order operator in (3.1) for the time variable leads to different equations to solve.

Taking  $\mathcal{D}_t = \mathcal{D}_t^+$ , one acquires the **explicit Euler scheme**:

$$\frac{U_i^{j+1} - U_i^j}{\Delta T} = \frac{U_{i+1}^j - 2U_i^j + U_{i-1}^j}{(\Delta X)^2} \quad (3.9)$$

Note that figure 2.1(b) is the numerical solution acquired using this scheme. While it is easy to compute the “next time step” by observing that this can be written as  $U_i^{j+1} = U_i^j + \frac{\Delta T}{(\Delta X)^2} (U_{i+1}^j - 2U_i^j + U_{i-1}^j)$  (where the RHS is known), a formal analysis using discrete Fourier transform shows that this scheme is stable if and only if  $\mu := \frac{\Delta T}{(\Delta X)^2} \leq \frac{1}{2}$ .

Conversely, taking  $\mathcal{D}_t = \mathcal{D}_t^-$ , one acquires the **implicit Euler scheme**:

$$\frac{U_i^j - U_i^{j-1}}{\Delta T} = \frac{U_{i+1}^j - 2U_i^j + U_{i-1}^j}{(\Delta X)^2} \quad (3.10)$$

which is unconditionally stable, but requires solving a nonlinear equation to acquire the next step. For more detail, see [10].

## 4 Tangent-Point Energy

Given a curve  $\gamma : M \rightarrow \mathbb{R}^3$ , a sensible choice of curve energy is the tangent-point energy[12].

**Definition** (Tangent-Point Energy). For a continuously differentiable parameterised curve  $\gamma : M \rightarrow \mathbb{R}^3$ , define **tangent-point energy** (TPE) as:

$$\mathcal{E}_\beta^\alpha(\gamma) := \iint_{M^2} k_\beta^\alpha(\gamma_x, \gamma_y, \mathbf{T}_x) d\gamma_x d\gamma_y \quad (4.1)$$

where  $\mathbf{T}_x := \frac{d\gamma_x}{dt} / \left| \frac{d\gamma_x}{dt} \right|$  is the unit tangent vector at  $\gamma_x$  along the curve, and **tangent-point kernel** is given as:

$$k_\beta^\alpha(\mathbf{p}, \mathbf{q}, \mathbf{T}) := \frac{|\mathbf{T} \wedge (\mathbf{p} - \mathbf{q})|^\alpha}{|\mathbf{p} - \mathbf{q}|^\beta} \quad (4.2)$$

$\alpha$  and  $\beta$  are parameters one could choose, but for tangent-point energy to be well-defined, one may choose them to satisfy  $\alpha > 1$  and  $\beta \in [\alpha + 2, 2\alpha + 1]$ . The intuition is that TPE takes not only the displacement between two points, but its relation to the tangent vector via cross product, “controlling” the strength of singularity.

Note that choosing  $\alpha = 2$  and  $\beta = 4$  results in the scaled version of the original TPE by Buck and Orloff[4].

The choice of parameters  $\alpha$  and  $\beta$  changes the behaviour of the tangent-point energy as stated in the following lemma.

**Lemma 4.1.** *Tangent-point energy  $\mathcal{E}_\beta^\alpha$  defined as (4.1) is scale invariant with respect to the curve if and only if  $\beta = \alpha + 2$ . Moreover, if  $\beta > \alpha + 2$ , then  $\mathcal{E}_\beta^\alpha$  scales inversely with the curve.*

*Proof.* Take a parameterised curve  $\gamma : M \rightarrow \mathbb{R}^3$  and  $\Gamma := c\gamma$ , a curve scaled by factor  $c > 0$  of  $\gamma$ . Note that the unit tangent vector is identical for  $\gamma$  and  $\Gamma$ , that is,  $\mathbf{T}_x := \frac{d\gamma_x}{dt} / \left| \frac{d\gamma_x}{dt} \right| = \frac{d\Gamma_x}{dt} / \left| \frac{d\Gamma_x}{dt} \right|$

Then,

$$\frac{k_\beta^\alpha(\gamma_x, \gamma_y, \mathbf{T}_x)}{k_\beta^\alpha(\Gamma_x, \Gamma_y, \mathbf{T}_x)} = \frac{|\gamma_x - \gamma_y|^\alpha}{|\Gamma_x - \Gamma_y|^\beta} = c^{\beta-\alpha} \quad (4.3)$$

Also note that

$$d\Gamma = c d\gamma \quad (4.4)$$

So, we deduce from (4.1),

$$\mathcal{E}_\beta^\alpha(\Gamma) = c^{\alpha-\beta+2} \mathcal{E}_\beta^\alpha(\gamma) \quad (4.5)$$

Hence,  $\mathcal{E}_\beta^\alpha$  is scale invariant with respect to the curve if and only if  $\alpha - \beta + 2 = 0$ , and if  $\beta > \alpha + 2$ ,  $\mathcal{E}_\beta^\alpha$  scales as  $O\left(\frac{1}{c^{\beta-(\alpha+2)}}\right)$  as  $c \rightarrow \infty$ . ■

*Remark.* If  $\beta < \alpha + 2$ , then the energy scales with the size of the curve, meaning that the energy is trivially minimised by scaling down the curve to a singularity, which is not desirable in our context.

One could also justify the condition on  $\alpha$  and  $\beta$  by the following lemma.

**Lemma 4.2.** *Given  $\alpha$  and  $\beta$ , the singularity of the kernel at a point and another point of which is arc-length  $\epsilon > 0$  away from it is of order  $O(\epsilon^{2\alpha-\beta})$ , that is,  $k_\beta^\alpha(\gamma(s), \gamma(s+\epsilon), \mathbf{T}(s)) = O(\epsilon^{2\alpha-\beta})$  as  $\epsilon \rightarrow 0$ . Moreover, if  $2\alpha = \beta$ , then the kernel converges to  $(\frac{\kappa}{2})^\alpha$  as the two points get closer, where  $\kappa$  is the curvature of the curve at the point.*

*Proof.* For  $\gamma(s) = (x(s), y(s), z(s))$  parameterised by arc-length, one recognises that the tangent vector at this point is  $\mathbf{T} = \gamma'(s)$ . Note that  $|\gamma'(s)| = |\mathbf{T}| = 1$ .

By Taylor expansion:

$$\gamma(s+\epsilon) = \gamma(s) + \epsilon\gamma'(s) + \frac{1}{2}\epsilon^2\gamma''(s) + O(\epsilon^3) \quad (4.6)$$

Then around  $\epsilon = 0$ ,

$$\begin{aligned} k_\beta^\alpha(\gamma(s), \gamma(s+\epsilon), \gamma'(s)) &= \frac{|\gamma'(s) \wedge (\gamma(s+\epsilon) - \gamma(s))|^\alpha}{|\gamma(s+\epsilon) - \gamma(s)|^\beta} \\ &= \frac{|\gamma'(s) \wedge (\epsilon\gamma'(s) + \frac{1}{2}\epsilon^2\gamma''(s) + O(\epsilon^3))|^\alpha}{|\epsilon\gamma'(s) + O(\epsilon^2)|^\beta} \\ &= \frac{\epsilon^{2\alpha-\beta} |\gamma'(s) \wedge \gamma''(s) + O(\epsilon)|^\alpha}{2^\alpha |\gamma'(s) + O(\epsilon)|^\beta} \\ &= \frac{\epsilon^{2\alpha-\beta}}{2^\alpha} \left( \frac{|\gamma'(s)|^\alpha |\gamma''(s)|^\alpha}{|\gamma'(s)|^\beta} + O(\epsilon) \right) \\ &= \frac{\epsilon^{2\alpha-\beta}}{2^\alpha} (\kappa^\alpha + O(\epsilon)) \end{aligned}$$

$\because \gamma'(s) \wedge \gamma'(s) = \mathbf{0}$   
 $\because \gamma'(s) \perp \gamma''(s)$   
 $\because |\gamma'(s)| = |\mathbf{T}| = 1$   
 and  $|\gamma''(s)| = \kappa$

So with arc-length perturbation of  $\epsilon$ , the order of singularity of the kernel is  $O(\epsilon^{2\alpha-\beta})$ . In particular, if  $2\alpha - \beta = 0$ , the kernel converges to  $(\frac{\kappa}{2})^\alpha$  (Figure 4.2(a)). ■

*Remark.* The geometric intuition of  $k_4^2$  (“Buck-Orloff kernel”), for example, is that  $k_4^2(\gamma_x, \gamma_y, \mathbf{T}_x)$  evaluates to  $\frac{1}{4r^2}$  where  $r$  is the radius of the smallest circle drawn that is tangent to the curve at  $\gamma_x$  and passes through  $\gamma_y$  (Figure 4.1). Taking  $\gamma_y \rightarrow \gamma_x$ , lemma 4.2 is consistent with the intuition that  $k_4^2(\gamma_x, \gamma_y, \mathbf{T}_x) \rightarrow \frac{\kappa^2}{4}$  where  $\kappa$  is the curvature at  $\gamma_x$ .<sup>5</sup> (Figure 4.2(a))

From lemma 4.1 and lemma 4.2, the well-definedness condition of TPE follows from arguing by integrability of functions with isolated poles of order lower than 1. (Figure 4.3)

---

<sup>5</sup>Can be considered “removable singularity” (Figure 4.2(b))

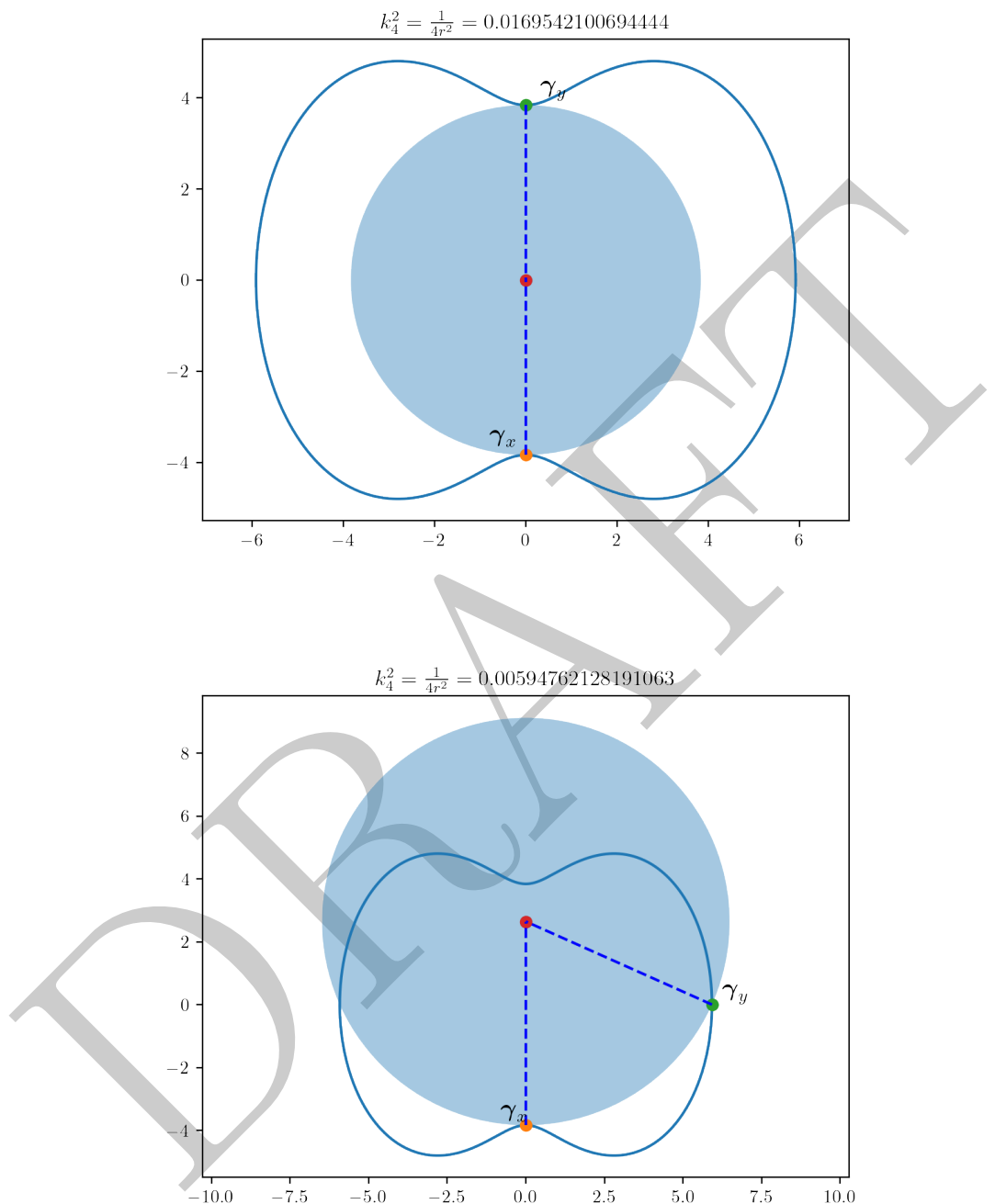


Figure 4.1: Intuition behind  $k_4^2$

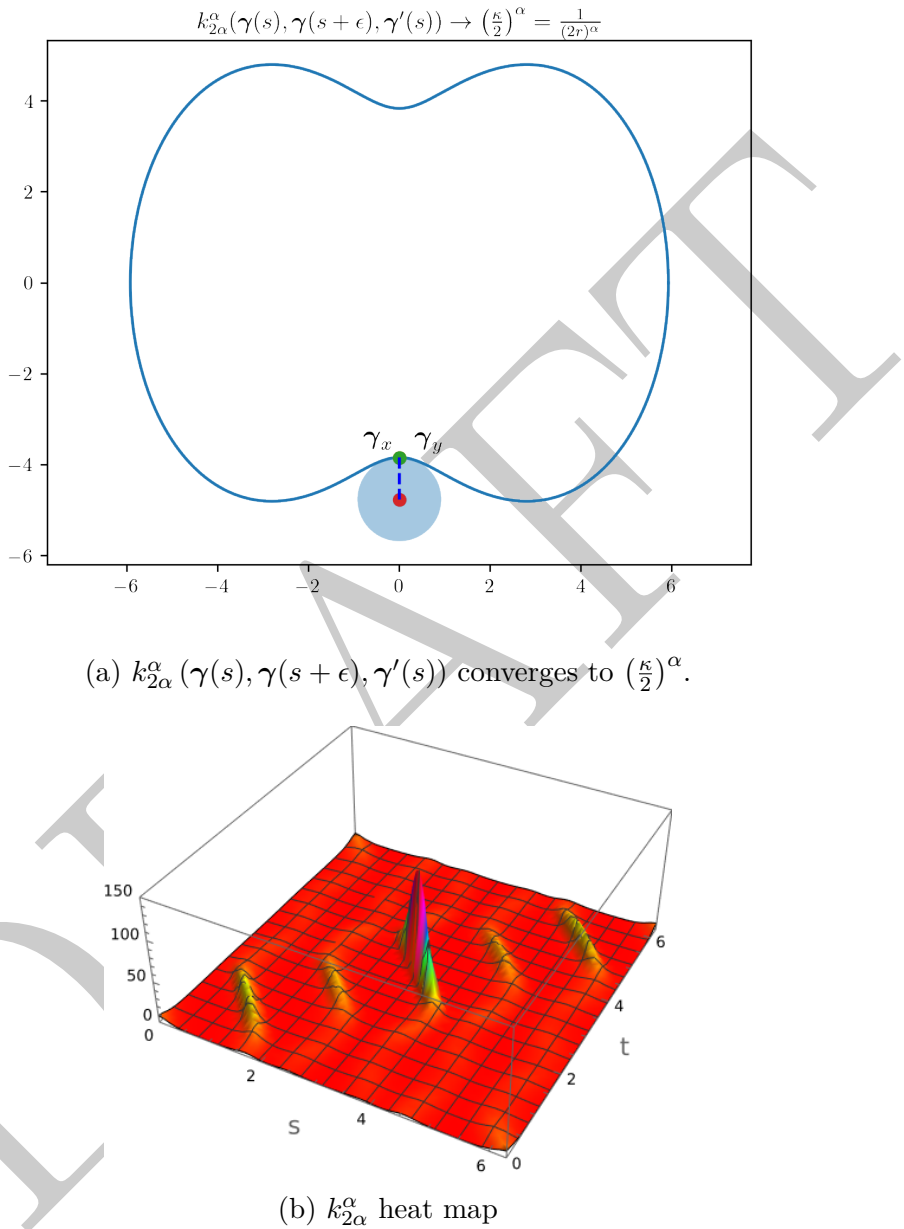


Figure 4.2: Behaviours of  $\beta = 2\alpha$  kernel



Figure 4.3: Heat map of  $k_{4,5}^2$ : Even with singularities, because it is weaker than  $O\left(\frac{1}{\epsilon}\right)$ , the kernel is integrable, hence  $\mathcal{E}_{4,5}^2$  is well-defined.

**Corollary 4.3.** *If  $\alpha > 1$  and  $\beta \in [\alpha + 2, 2\alpha + 1]$ , tangent-point energy  $\mathcal{E}_\beta^\alpha$  is well-defined.*

*Remark.* Ideas from lemma 4.1 and lemma 4.2 suggest that modification of the naïvely introduced energy kernel  $k_S(\gamma_1, \gamma_2) = \frac{1}{|\gamma_1 - \gamma_2|}$  to  $\tilde{k}_S(\gamma_1, \gamma_2) = \frac{1}{|\gamma_1 - \gamma_2|^p}$  is not feasible. By choosing  $p < 1$ , singular behaviour is  $O(1/\epsilon^p)$  as  $\epsilon \rightarrow 0$  hence integrable, but a similar analysis to lemma 4.1 shows that one needs to take  $p \geq 2$  for the energy not to be scale proportional to the scaling of the curve. Hence, the kernel  $\tilde{k}_S$  is still ill-defined.

## 5 Unknotting Curves via Gradient Flow Equation

Now that gradient flow equation and tangent-point energy are introduced, one formalises the process of untangling a curve:

**Definition** (Curve Untangling Process). Given a parameterised curve  $\gamma : M \times T \rightarrow \mathbb{R}^3$  over an interval  $M$  and time domain  $T$ , denote the following initial value problem as **curve untangling process**:

$$\frac{\partial \gamma}{\partial t} = -\text{grad}_\gamma \mathcal{E}_\beta^\alpha(\gamma) - \text{grad}_\gamma \mathcal{C}(\gamma) \quad (5.1)$$

$$\gamma(s; 0) = \gamma_0(s) \quad (5.2)$$

where

- $\gamma_0(s)$  is the parameterisation of the initial (tangled) curve.
- $\mathcal{E}_\beta^\alpha$  is the tangent-point energy (See (4.1))
- $\mathcal{C}$  is additional constraint energy to control behaviour of curve untangling process. (See section 5.2.1.)

## 5.1 Discretisation for Numerical Computation

Solving (5.1), (5.2) analytically is challenging. Rather, we aim to acquire a numerical solution. Assume for simplicity that the curve of interest is simple closed.<sup>6</sup>

### 5.1.1 Discretisation of Curve

We start by discretising the initial curve  $\gamma_0$  by taking  $N$  points on a curve as shown in Figure 5.1. Represent the initially discretised curve in the form of multidimensional array (or a matrix for specific time step index):  $\Gamma^0 = (\mathbf{x}_0^0, \mathbf{x}_1^0, \dots, \mathbf{x}_{N-1}^0) \in \mathbb{R}^{3 \times N}$ , and the discretised curve at subsequent time step  $k \in \mathbb{N} \cup \{0\}$  as  $\Gamma^k = (\mathbf{x}_0^k, \mathbf{x}_1^k, \dots, \mathbf{x}_{N-1}^k) \in \mathbb{R}^{3 \times N}$ . Since we restrict our attention to a simple closed curve, it is convenient to extend the indexing rule by:

$$\mathbf{x}_i^k = \mathbf{x}_{r(i,N)}^k \quad \text{where } r(i,N) = (\text{remainder of } i \div N) \quad (5.3)$$

so that  $\mathbf{x}_N^k = \mathbf{x}_0^k$ ,  $\mathbf{x}_{N+1}^k = \mathbf{x}_1^k$ , etc.

Define (right) operator  $[\cdot] : \mathbb{R}^{3 \times N} \rightarrow \mathbb{R}$  such that for array  $T \in \mathbb{R}^{3 \times N}$ ,

$$T[i] := T \mathbf{e}_{r(i,N)}$$

where  $\mathbf{e}_i$  is the  $i^{\text{th}}$  canonical vector. With this operator, one could write

$$\Gamma^k[i] = \mathbf{x}_{r(i,N)}^k = \mathbf{x}_i^k \quad (5.4)$$

analogous to  $\gamma = \gamma(s; t)$  being a parameterised curve, which is a vector-valued function.

Finally, denote by  $e_i^k$  for the (undirected) edge with vertex pair  $(\mathbf{x}_i^k, \mathbf{x}_{i+1}^k)$ .

### 5.1.2 Discretisation of Tangent-Point Energy

In order to acquire numerical solution, one must also be able to numerically compute the TPE. For this, we pose the energy quadrature  $E_\beta^\alpha(\Gamma^k)$  of the following form:

$$\mathcal{E}_\beta^\alpha(\gamma(\cdot, t)) := \iint_{M^2} k_\beta^\alpha(\gamma_x, \gamma_y) d\gamma_x d\gamma_y \approx E_\beta^\alpha(\Gamma^k) := \sum_{i,j \in \{0, \dots, N-1\}} K_\beta^\alpha(i, j) |e_i^k| |e_j^k| \quad (5.5)$$

where  $K_\beta^\alpha$  is an approximation of tangent-point kernel  $k_\beta^\alpha$  (which is specified at (5.6)), and  $|e_i^k|$  is the length of edge  $e_i^k$ , that is,  $|e_i^k| = |\mathbf{x}_i^{k+1} - \mathbf{x}_i^k|$ . Note that  $\Gamma^k$  is a polygonal curve, for which TPE (4.1) is not well-defined due to locally non-integrable contributions from vertices:

One way to resolve the issue is to “ignore” the adjacent edge contribution[12] in the energy quadrature  $E_\beta^\alpha$  as in Figure 5.2(a). The justification is that as we take a finer mesh ( $N$  sufficiently large), the product of edge lengths ( $|e_i| |e_j|$ ) should tend to

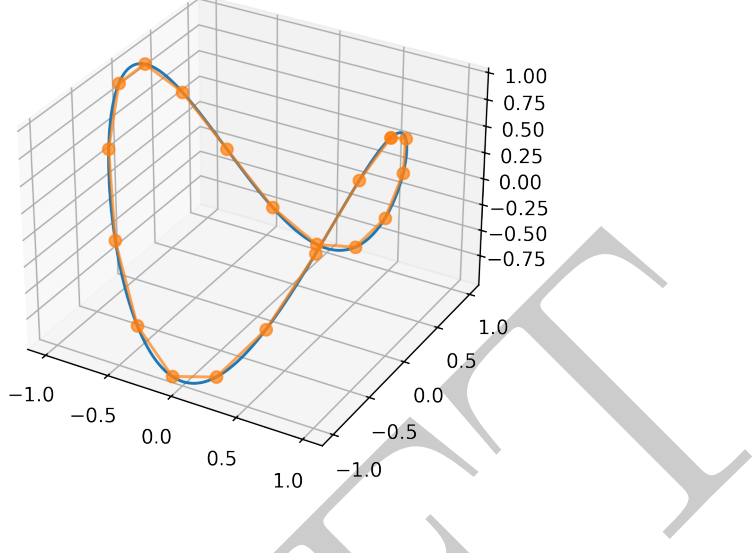


Figure 5.1: Discretisation of a simple closed curve by sampling the points along the curve.

zero sufficiently fast, resulting in approximation of the energy for the smooth curve, which did not have vertices resulting in local non-integrability in the first place.

It still remains to sensibly approximate the kernel  $k_\beta^\alpha(\gamma_x, \gamma_y) \approx K_\beta^\alpha(i, j)$ . One sensible approximation is to use the following 4-point quadrature[12].

$$K_\beta^\alpha(i, j) := \frac{1}{4} \left( k_\beta^\alpha(\mathbf{x}_i^k, \mathbf{x}_j^k, \mathbf{T}_i^k) + k_\beta^\alpha(\mathbf{x}_i^k, \mathbf{x}_{j+1}^k, \mathbf{T}_i^k) + k_\beta^\alpha(\mathbf{x}_{i+1}^k, \mathbf{x}_j^k, \mathbf{T}_i^k) + k_\beta^\alpha(\mathbf{x}_{i+1}^k, \mathbf{x}_{j+1}^k, \mathbf{T}_i^k) \right) \quad (5.6)$$

where  $\mathbf{T}_i^k := \frac{\mathbf{x}_{i+1}^k - \mathbf{x}_i^k}{|\mathbf{x}_{i+1}^k - \mathbf{x}_i^k|}$  approximates the tangent vector to the curve at  $\gamma_x$ . (See Figure 5.2(b).)

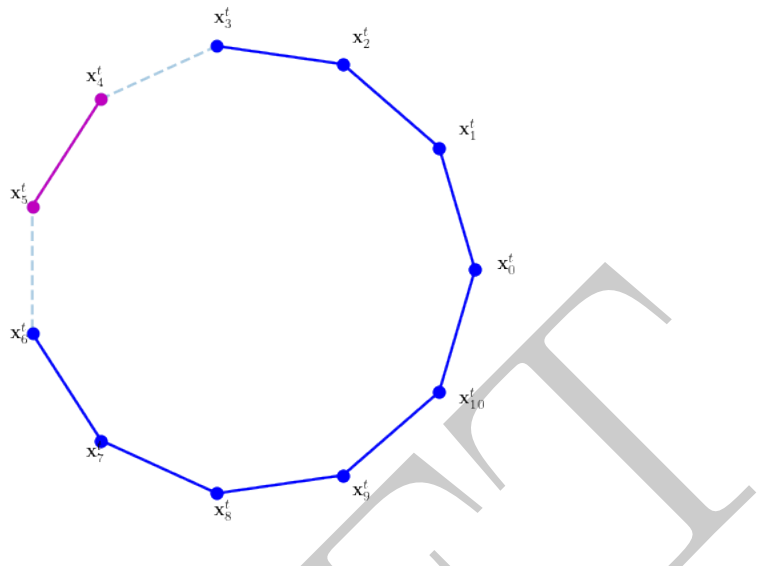
Putting (5.5) and (5.6) together, one can write the **tangent-point energy quadrature** as:

$$E_\beta^\alpha(\Gamma^k) := \sum_{\substack{i,j \in \{0, \dots, N-1\} \\ r(i-j, N) > 1}} K_\beta^\alpha(i, j) |e_i^k| |e_j^k| \quad (5.7)$$

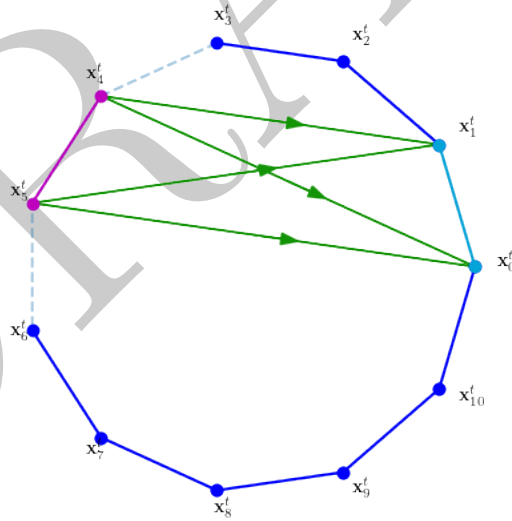
where  $r(i-j, N)$  is the geodesic distance between  $i$  and  $j$  in modulo  $N$ . For discussion of quadratures for nonclosed curves, see appendix C.

---

<sup>6</sup>We may assume that the function definition of  $\gamma : M \rightarrow \mathbb{R}^3$  extends to  $\gamma : \mathbb{R} \rightarrow \mathbb{R}^3$  by periodicity.



(a) For a chosen edge  $e_i^k$ , we ignore the two adjacent edges  $e_{i-1}^k$ ,  $e_{i+1}^k$ . In the limit as  $N \rightarrow 0$ , because the edge lengths tend to zero, the discrepancy between the quadrature and the analytical value of the energy is expected to tend to zero.



(b) Tangent-point kernel is approximated by 4-point quadrature defined as (5.6).

Figure 5.2: Quadrature for approximation of TPE.

### 5.1.3 Derivative Operators Discretised Curve

For discrete curve, the (forward and backward) first derivative operators (2.13) transforms to operator for  $U(\Gamma^k[\cdot]) : \{0, 1, \dots, N-1\} \rightarrow \mathbb{R}$  characterised by:

$$\tilde{\nabla}_{\Gamma^k}^+ U(\Gamma^k[i]) = \frac{U(\Gamma^k[i+1]) - U(\Gamma^k[i])}{|\Gamma^k[i+1] - \Gamma^k[i]|} \mathbf{T}_i^k \quad (5.8)$$

$$\tilde{\nabla}_{\Gamma^k}^- U(\Gamma^k[i]) = \frac{U(\Gamma^k[i]) - U(\Gamma^k[i-1])}{|\Gamma^k[i] - \Gamma^k[i-1]|} \mathbf{T}_{i-1}^k \quad (5.9)$$

and analogously with second derivative operator:

$$\tilde{\Delta}_{\Gamma^k} U(\Gamma^k[i]) = \frac{\frac{U(\Gamma^k[i+1]) - U(\Gamma^k[i])}{|\Gamma^k[i+1] - \Gamma^k[i]|} - \frac{U(\Gamma^k[i]) - U(\Gamma^k[i-1])}{|\Gamma^k[i] - \Gamma^k[i-1]|}}{\frac{1}{2} |\Gamma^k[i+1] - \Gamma^k[i-1]|} \quad (5.10)$$

$$= \frac{|e_i| U_{i-1} - (|e_{i-1}| + |e_i|) U_i + |e_{i-1}| U_{i+1}}{|e_{i-1}| |e_i| |f_i|} \quad (5.11)$$

$$= \frac{1}{|e_{i-1}| |e_i| |f_i|} \begin{pmatrix} |e_i| & -(|e_{i-1}| + |e_i|) & |e_{i-1}| \end{pmatrix} \begin{pmatrix} U_{i-1} \\ U_i \\ U_{i+1} \end{pmatrix} \quad (5.12)$$

where one defines  $f_i := \frac{1}{2} (\Gamma^k[i+1] - \Gamma^k[i-1])$  and  $U_i := U(\Gamma^k[i])$ .

However, inverting the Laplacian is troublesome, as it is equivalent to inverting a singular matrix as stated in the following lemma.

**Lemma 5.1.** *The matrix capturing curve Laplacian  $\tilde{\Delta}_{\Gamma^k}$  for closed discrete curve  $\Gamma^k$  is singular.*

*Proof.* The matrix  $L$  for  $\tilde{\Delta}_{\Gamma^k}$  for closed discrete curve  $\Gamma^k$  has the form:

$$L := \begin{pmatrix} * & * & & & * \\ * & * & * & & \\ * & * & * & & \\ \ddots & \ddots & \ddots & & \\ * & * & * & * & * \\ * & * & * & * & * \end{pmatrix}$$

To show that  $L$  is singular, it is sufficient to show that there is a nontrivial solution  $\mathbf{x}$  to  $L\mathbf{x} = \mathbf{0}$ . Since rows follow from (5.12), observe that the rows sum to zero. Hence, one can spot such nontrivial solution  $\mathbf{x} = (1, 1, \dots, 1)^T$ . ■

In order to proceed, one needs to “regularise” the Laplacian to make it invertible as in section 5.3.

### 5.1.4 Finite Difference Scheme of Curve Untangling Process

Based on (5.1), one writes the following finite difference scheme:

$$\mathcal{D}_t \boldsymbol{\Gamma}^k = -\text{Grad}_X E_\beta^\alpha(\boldsymbol{\Gamma}^k) - \text{Grad}_X C(\boldsymbol{\Gamma}^k) \quad \text{for } k = 0, 1, \dots \quad (5.13)$$

where  $\mathcal{D}_t$  is the finite difference operator over time,  $\text{Grad}_X$  is discrete equivalent<sup>7</sup> of  $\text{grad}_X$  on discrete inner product space  $X$  (which may be omitted in the notation),  $E_\beta^\alpha$  is the TPE quadrature defined as (5.7), and  $C$  is the discretisation of the constraint energy  $\mathcal{C}$  (See section 5.2.1). Often times, however, it is easier to construct finite difference scheme directly from (5.1) after some simplification, rather than attempting to use (5.13) directly. Note that because similar operations are done for each point vector, this is a parallelisable task. For the simplest scheme, one could take the forward difference operator characterised as  $\mathcal{D}_t^+ \boldsymbol{\Gamma}^k[i] := \frac{\boldsymbol{\Gamma}^{k+1}[i] - \boldsymbol{\Gamma}^k[i]}{\Delta T}$ .

## 5.2 Example: $L^2$ Explicit Euler Scheme

Now we visit the simplest numerical scheme for curve untangling process. Assume for now scale-invariance by taking parameters  $\alpha$  and  $\beta$  to satisfy  $\beta = \alpha + 2$  (See lemma 4.1).

In  $L^2$ ,  $\text{grad}_{L^2} \mathcal{E}_\beta^\alpha(\boldsymbol{\gamma})$  is simply the “first-order perturbation” as in (2.6). Discrete equivalent is the  $\ell^2$  space, where one justifies this by noting that first-order perturbation in a curve is analogous to perturbing each point of its discretisation. Taking  $\mathcal{D}_t = \mathcal{D}_t^+$  from (5.13),

$$\frac{\boldsymbol{\Gamma}^{k+1} - \boldsymbol{\Gamma}^k}{\Delta T} = -\text{Grad}_{\ell^2} E_\beta^\alpha(\boldsymbol{\Gamma}^k) \quad (5.14)$$

where one could explicitly write  $\text{Grad}_{\ell^2} E_\beta^\alpha(\boldsymbol{\Gamma}^k)$  as

$$\text{Grad}_{\ell^2} E_\beta^\alpha(\boldsymbol{\Gamma}^k) = \underbrace{\begin{pmatrix} \frac{\partial}{\partial x_{1,1}} & \frac{\partial}{\partial x_{1,2}} & \cdots & \frac{\partial}{\partial x_{1,N-1}} \\ \frac{\partial}{\partial x_{2,1}} & \frac{\partial}{\partial x_{2,2}} & \cdots & \frac{\partial}{\partial x_{2,N-1}} \\ \frac{\partial}{\partial x_{3,1}} & \frac{\partial}{\partial x_{3,2}} & \cdots & \frac{\partial}{\partial x_{3,N-1}} \end{pmatrix}}_{\nabla_{\boldsymbol{\Gamma}^k}} E_\beta^\alpha(\boldsymbol{\Gamma}^k) \in \mathbb{R}^{3 \times N} \quad (5.15)$$

where  $x_{j,i}$  refers to the  $(j, i)$  coordinate variable for  $3 \times N$  array.

*Remark.*  $\text{Grad}_{\ell^2}$  is in fact a linear operator with respect to its input, energy.

One could use this exact form of  $\text{Grad}_{\ell^2} E_\beta^\alpha(\boldsymbol{\Gamma}^k)$  as given in appendix D, but it could be considered cumbersome (even though there are benefits to implementing this as stated in section 5.2.2). One could alternatively approximate  $\text{Grad}_{\ell^2} E_\beta^\alpha(\boldsymbol{\Gamma}^k)$  by central difference scheme, for example: for  $i = 0, 1, \dots, N-1$  and  $j = 1, 2, 3$ ,

$$\mathbf{e}_j \cdot (\text{Grad}_{\ell^2} E_\beta^\alpha(\boldsymbol{\Gamma}^k)[i]) = \frac{\partial E_\beta^\alpha(\boldsymbol{\Gamma}^k)}{\partial x_{j,i}} \approx \frac{1}{2\Delta X} (\bar{E}_\beta^\alpha(i, j, k) - \underline{E}_\beta^\alpha(i, j, k)) \quad (5.16)$$

---

<sup>7</sup>Worth noting that  $\text{Grad}_X : \mathbb{T} \rightarrow \mathbb{T}$  where  $\mathbb{T}$  is a set of arrays of certain shape;  $\text{Grad}_X$  maps arrays to arrays of the same shape.



Figure 5.3:  $-\text{Grad}_{L^2}(\Gamma^k)$  which is the direction of flow of a discretised curve  $\Gamma^k$  at each point, represented by the arrows. The magnitude is represented by both color and the length of the arrows.



Figure 5.4:  $L^2$  gradient flow on a figure-eight curve. Note that there are “sharp” points, along with “high frequency oscillation” (which are undesirable or unexpected characteristics); this may be due to the fact that  $L^2$  gradient flow does not take the smoothness of the curve into account.

where

$$\begin{aligned}\bar{E}_\beta^\alpha(i, j, k) &:= E_\beta^\alpha \left( (\mathbf{x}_0^k, \dots, \mathbf{x}_{i-1}^k, \mathbf{x}_i^k + \Delta X \mathbf{e}_j, \mathbf{x}_{i+1}^k, \dots, \mathbf{x}_{N-1}^k) \right) \\ \underline{E}_\beta^\alpha(i, j, k) &:= E_\beta^\alpha \left( (\mathbf{x}_0^k, \dots, \mathbf{x}_{i-1}^k, \mathbf{x}_i^k - \Delta X \mathbf{e}_j, \mathbf{x}_{i+1}^k, \dots, \mathbf{x}_{N-1}^k) \right)\end{aligned}$$

See Figure 5.4 for a demonstration of curve untangling process using this  $L^2$  gradient. Note that because  $L^2$  gradient flow does not take smoothness into account, this may break the assumption later of the smoothness of the curve, which could be problematic as the TPE quadrature relied on the assumption that the discrete curve stays “relatively smooth”.

*Remark.* Notice that (5.14) can be interpreted as SDM over all the coordinates on the curve! This is consistent with the motivation of gradient flow equation given in section 2.1.

There is another subtlety; there is no guarantee that the edge lengths do not grow, which could break the assumption that the TPE quadrature is valid. This can be mitigated by prescribing edge lengths  $L_i$  using some constraint energy as in section 5.2.1.

We now attempt the finite difference scheme with a *scale-variant energy*, that is, when  $\beta > \alpha + 2$ . If one attempts the same finite difference scheme as (5.14) one may observe that the curve “grows” in size, indefinitely. This is due to the fact that with  $\beta > \alpha + 2$ , by the virtue of lemma 4.1, energy scales inversely proportional to its scale factor (Figure 5.5). To use scale-variant energy, one may consider having constraint energy as part of the curve untangling process.

### 5.2.1 Constraint Energy

From lemma 4.1 and as demonstrated in Figure 5.5, in the case that  $\beta > \alpha + 2$ , one could trivially minimise TPE  $\mathcal{E}_\beta^\alpha$  of the curve (and by the same logic,  $E_\beta^\alpha$  of the

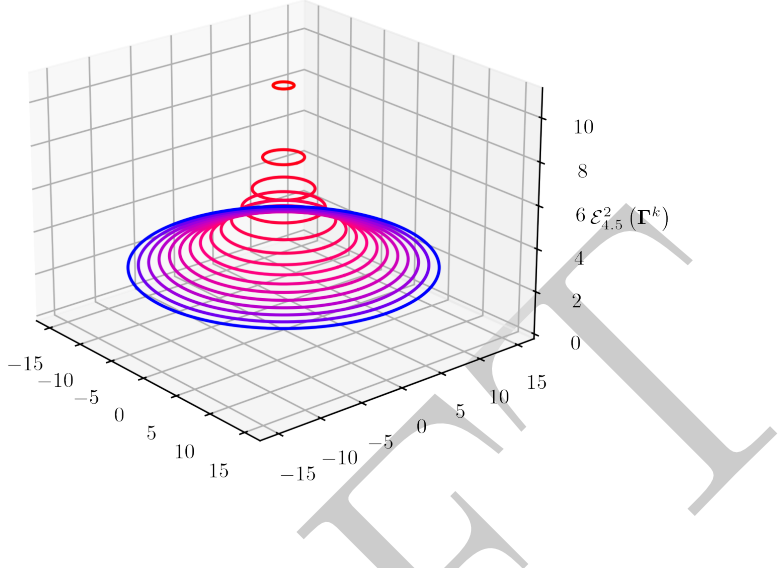


Figure 5.5: The height represents  $\mathcal{E}_{4,5}^2$  for circles of different radius. Note that the energy decreases trivially by taking a larger circle.

discretised curve, albeit due to increases in edge lengths, would cease to be a “valid” quadrature) by scaling the curve to infinity. In order to avoid this phenomenon, or to change the behaviour of the flow, one may add additional energy penalising unwanted behaviours.

Here are some examples of constraint one could take. (Since we are interested in numerical schemes, constraints are expressed for  $C$  rather than  $\mathcal{C}$ .)

- Taking  $C(\Gamma^k) := \lambda \sum_{i=0}^{N-1} |\Gamma^k[i]|^p$  adds the motivation for the curve not to stray away from the origin.
- Taking  $C(\Gamma^k) := \lambda \left| \sum_{i=0}^{N-1} |e_i| - L \right|^p$  adds the motivation for the curve to stay close to some constant arc-length  $L$ .
- Taking  $C(\Gamma^k) := \lambda \sum_{i=0}^{N-1} ||e_i| - L_i|^p$  adds the motivation for the edge lengths on the discretised curve not to deviate from prescribed edge lengths  $L_i$ .

$\lambda \geq 0$  is the strength of the overall constraint, and  $p > 0$  is the order of “thresholding”, where higher  $p$  would lead to harsher “thresholding”.

### 5.2.2 Time Complexity

Since we expect to take  $N$  to be very large, it is reasonable to consider the computational work.

If we use a difference scheme to approximate  $\text{Grad}_{\ell^2} E_{\beta}^{\alpha}(\boldsymbol{\Gamma}^k)$ , for every time step, one needs to be able to evaluate  $E_{\beta}^{\alpha}$  for a given  $\boldsymbol{\Gamma}^k \in \mathbb{R}^{3 \times N}$ . From (5.7), it takes  $O(N^2)$  evaluations of the kernel. Since the approximation for  $\text{Grad}_{L^2} E_{\beta}^{\alpha}$  requires evaluation of the energy for each point perturbed, it takes  $O(N^3)$  evaluations of the kernel for each time step.

On the other hand, this is where doing the hard work of implementing *exact gradient computation* as in Appendix D is beneficial. For exact gradient implementation as in appendix D, it takes  $O(N)$  evaluations<sup>8</sup> of the derivative of the kernel. This implies the overall computation needed for a single step is  $O(N^2)$ .

### 5.2.3 Discussion of Implicit $L^2$ Euler

A problem with explicit schemes is that, there often exists some sort of condition for stability. (See section 3.2)

For unconditional stability, one may attempt implicit Euler scheme, that is, taking  $\mathcal{D}_t = \mathcal{D}_t^-$  in (5.13),

$$\frac{\boldsymbol{\Gamma}^k - \boldsymbol{\Gamma}^{k-1}}{\Delta T} = -\text{Grad}_{\ell^2} E_{\beta}^{\alpha}(\boldsymbol{\Gamma}^k) \quad (5.17)$$

This scheme however involves solving a nonlinear equation. One needs an efficient rootfinding algorithm (such as Newton's method) to compute each time step.

We will stick to explicit Euler scheme for simplicity from now on.

## 5.3 Example: Euler Scheme in $H^{-1}$ and $H^1$

Consider curve untangling process in  $H^{-1}$ . By (2.9), we may write  $\text{grad}_{H^{-1}} \mathcal{E}_{\beta}^{\alpha}(\boldsymbol{\gamma}) = -\tilde{\Delta}_{\boldsymbol{\gamma}} (\text{grad}_{L^2} \mathcal{E}_{\beta}^{\alpha}(\boldsymbol{\gamma}))$ . For the discrete equivalent, take

$$\text{Grad } E_{\beta}^{\alpha} = -\tilde{\Delta}_{\boldsymbol{\Gamma}^k} (\text{Grad}_{\ell^2} E_{\beta}^{\alpha}(\boldsymbol{\Gamma}^k)) = -\tilde{\Delta}_{\boldsymbol{\Gamma}^k} (\nabla_{\boldsymbol{\Gamma}^k} E_{\beta}^{\alpha}(\boldsymbol{\Gamma}^k)) \quad (5.18)$$

Note that computing “third derivative operator” could increase complexity of the scheme. In fact, if one approximates the Laplacian as (5.10), for each time step, it takes  $O(N^4)$  evaluations of the kernel, so the scheme becomes impractical.

Conversely, consider curve untangling process in  $H^1$ . By (2.7), we write  $\text{grad}_{H^1} \mathcal{E}_{\beta}^{\alpha}(\boldsymbol{\gamma}) = -\tilde{\Delta}_{\boldsymbol{\gamma}}^{-1} \text{grad}_{L^2} \mathcal{E}_{\beta}^{\alpha}$ , and (5.1) without constraint term can be written as:

$$\frac{\partial \boldsymbol{\gamma}}{\partial t} = \tilde{\Delta}_{\boldsymbol{\gamma}}^{-1} \text{grad}_{L^2} \mathcal{E}_{\beta}^{\alpha}(\boldsymbol{\gamma}) \quad (5.19)$$

Discretising this with forward difference for time, one gets  $H^1$  explicit Euler scheme:

$$\frac{\boldsymbol{\Gamma}^{k+1} - \boldsymbol{\Gamma}^k}{\Delta T} = \tilde{\Delta}_{\boldsymbol{\gamma}}^{-1} \nabla_{\boldsymbol{\Gamma}^k} E_{\beta}^{\alpha}(\boldsymbol{\Gamma}^k) \quad (5.20)$$

---

<sup>8</sup>4( $N - 3$ ) to be exact.

where  $\tilde{\Delta}_{\Gamma^k}$  is the Laplacian as given in (5.10), and  $\nabla_{\Gamma^k}$  is still the conventional gradient operator over all the coordinates of  $\Gamma^k$ . Note that by lemma 5.1, one needs to “regularise” the curve Laplacian; we do not attempt to solve for an exact  $H^1$  gradient, but rather a close one. To compute a step, one performs three steps:

1. Compute  $\nabla_{\Gamma^k} E_{\beta}^{\alpha}(\Gamma^k)$ .
2. Solve linear system  $\mathcal{L}\mathcal{G}^T = (\nabla_{\Gamma^k} E_{\beta}^{\alpha}(\Gamma^k))^T$  for  $\mathcal{G} \in \mathbb{R}^{3 \times N}$ 
  - $\mathcal{L} = \tilde{\Delta}_{\Gamma^k} + cI$  is the (almost tridiagonal by (5.12)) matrix capturing the “regularised” discrete curve Laplacian  $\tilde{\Delta}_{\Gamma^k}$ ; because curve Laplacian matrix alone is singular, the linear system would not have a unique solution, and the regularisation is to pick a sensible solution to the singular linear system.
  - $c \neq 0$  is a constant such that  $c$  closer to zero characterises “more  $H^1$ -like flow”, at the cost of higher conditioning number.
  - $\mathcal{G}$  represents the discrete time derivative, that is,  $\mathcal{G} = \frac{\Gamma^{k+1} - \Gamma^k}{\Delta T}$ .
3. Evolve by  $\Gamma^{k+1} = (\Delta T) \mathcal{G} + \Gamma^k$ .

Note that the linear system  $\mathcal{L}\mathcal{G}^T = (\nabla_{\Gamma^k} E_{\beta}^{\alpha}(\Gamma^k))^T$  has the following structure:

$$\underbrace{\begin{pmatrix} * & * & & & * \\ * & * & * & & \\ & * & * & * & \\ & & \ddots & \ddots & \\ & & & * & \\ & & & & * \\ * & & & & * \\ & & & & * \\ & & & & * \end{pmatrix}}_{\mathcal{L} \in \mathbb{R}^{N \times N}} \mathcal{G}^T = \underbrace{\begin{pmatrix} * & * & * \\ * & * & * \\ * & * & * \\ \vdots & \vdots & \vdots \\ * & * & * \\ * & * & * \\ * & * & * \end{pmatrix}}_{(\nabla_{\Gamma^k} E_{\beta}^{\alpha}(\Gamma^k))^T \in \mathbb{R}^{N \times 3}}$$

Because solving (cyclic tridiagonal) matrix equation  $\mathcal{L}\mathcal{G}^T = \nabla_{\Gamma^k} E_{\beta}^{\alpha}(\Gamma^k)$  costs  $O(N)$  by Gaussian elimination or otherwise[9], the cost of computing  $H^1$  gradient is dominated by the cost of computing  $\text{Grad}_{L^2} E_{\beta}^{\alpha}(\Gamma^k)$ .

Note that because  $H^1$  takes weak derivative into account, the direction of the flow is more aligned with its neighbours as shown in Figure 5.6 and hence, smoother flow as shown in Figure 5.7.

Also, because  $H^1$  gradient operator was closer to the “order of the differential” of the curve, the evolution is faster (Figure 5.8). See section 6.1.3 for a bit more detail.

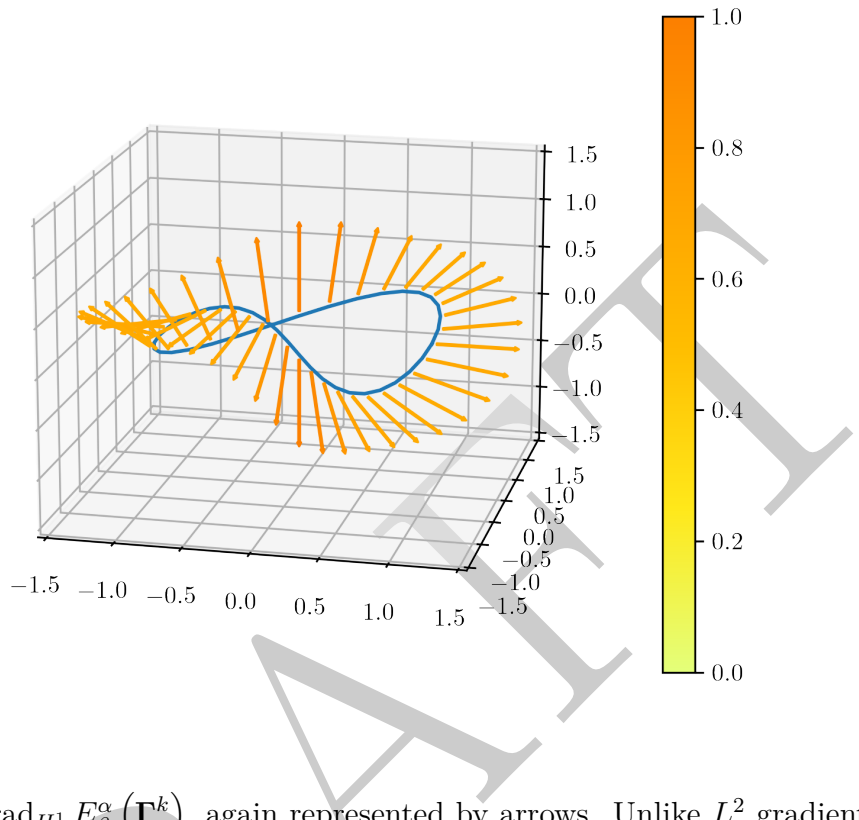


Figure 5.6:  $-\text{Grad}_{H^1} E_\beta^\alpha(\Gamma^k)$ , again represented by arrows. Unlike  $L^2$  gradient at Figure 5.3, direction of arrows are more aligned with its neighbours.

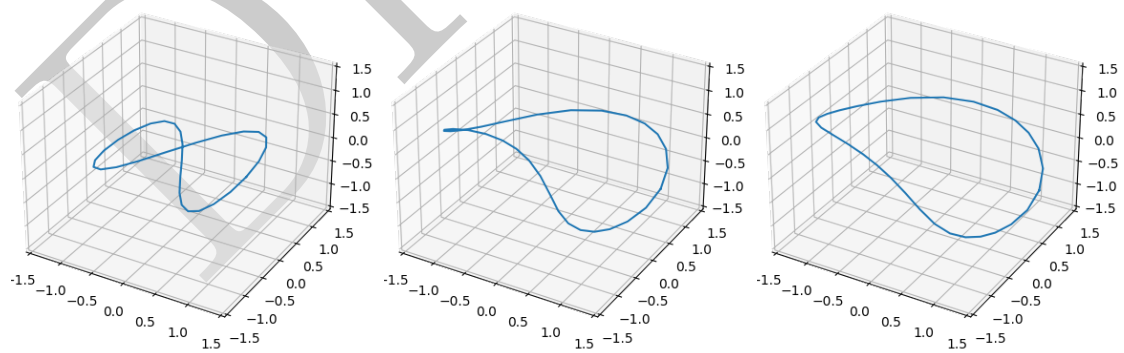


Figure 5.7:  $H^1$  flow on a figure-eight curve. Unlike  $L^2$  flow as shown in Figure 5.4,  $H^1$  takes the first derivative into account, hence results in a smoother curve.

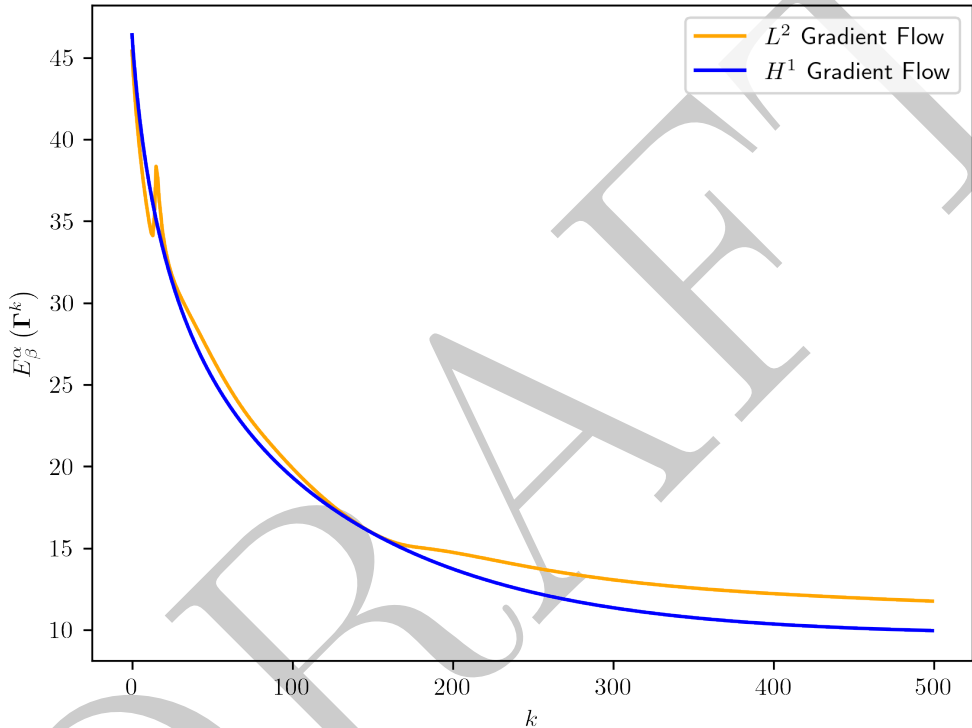


Figure 5.8: Untangling the figure-eight curve. Energy of the curve evolution in each gradient flow.  $H^1$  flow is more numerically stable as it avoids the excessive bending, forming a “sharp” point.

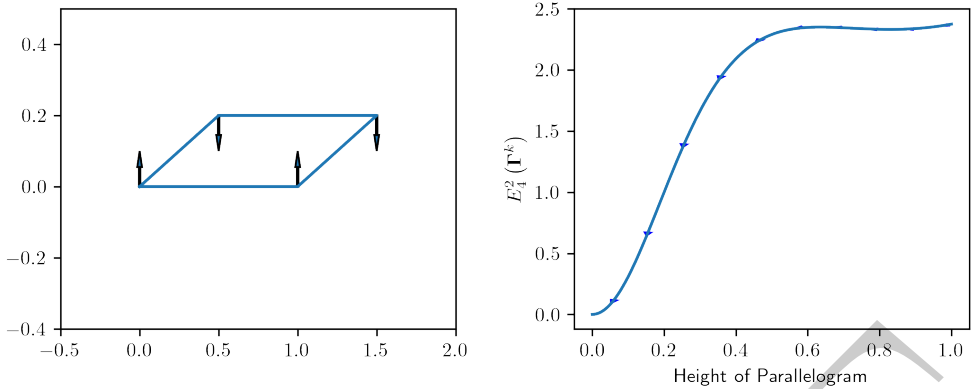


Figure 6.1: In the case of a 4-point discretised curve as shown, while computing the approximate kernel, it disregards the adjacent edges, which in fact takes significant portion of the curve out of consideration, and does not accurately approximate the kernel of the original curve. By taking the height of the parallelogram to zero, all the points align with all the edges  $e_i$ , hence energy is trivially reduced to zero.

## 6 Conclusion, Outlook, and Potential Alternative Approach

Because of the nature of discretisation, there is no absolute guarantee that a curve would not intersect; this implies that the implementation of the curve untangling process is not a trivial task, and must be carefully designed. Throughout experiments, common points of failure were:

- Some of the edge lengths of the discretised curve became sufficiently large that the quadrature ceased to become valid.
- The curves ceased to be smooth (as in Figure 5.4).
- The curves “collapsing” to nullify the kernel (Figure 6.1), usually after a long time since reaching a stationary state.
- Self-intersection in some cases.

The simplest idea to resolve some of the issues is to take a combination of appropriate constraints as in section 5.2.1 to steer the curve away from those issues. For example, the first point of failure could be fixed by taking the constraint of prescribing edge lengths to be the initial edge lengths. Of course, the others are innate to the approach itself, and one must modify the scheme to resolve them. The nonsmoothness issue can be resolved by using a higher order Sobolev space, nullification of the kernel can be resolved by stopping the evolution after achieving the energy value within a specified tolerance from the energy of the expected stationary state; for example, if one attempts evolution of curve which the unknot known to

---

**Algorithm 6.1** Modified backtracking Armijo line search

---

Choose constant  $0 < \delta < 1$ , and  $\Delta T^0$  such that after one step of evolution, the curve would not have crossed itself.

Let  $k = 0$ .

Choose  $M > 0$ , the number of time steps.

**while**  $k < M$  **do**

**if** evolution ( $\dagger$ ) by time step  $\Delta T^k$  requires self-crossing. **then**  
 $\Delta T^k \mapsto \delta \Delta T^k$ .

**else**

$$\Gamma^{k+1} := \underbrace{\Gamma^k - \Delta T^k (\text{Grad}_X E_\beta^\alpha(\Gamma^k) + \text{Grad}_X C(\Gamma^k))}_{(\dagger)}$$

$k \leftarrow k + 1$

**end if**

**end while**  $\triangleright$  One could choose any other appropriate condition for termination.

---

be a circle, with Buck-Orloff TPE  $\mathcal{E}_4^2$ , we stop the evolution after the energy of the curve is within some tolerance  $\epsilon > 0$  from  $\pi^2$ , the Buck-Orloff TPE of a circle. For the issue of self-intersection, it turns out that in practice, taking higher resolution and smaller time step help alleviate it, yet does not guarantee a complete fix.

Of course, there are alternative approaches of ameliorating the process of evolution.

## 6.1 Possible Variations to Curve Untangling Process

The most obvious way to improve the evolution is to take smaller time step and higher resolution of the curve. However, reducing the time step means the evolution itself will be slower, and increasing resolution means the computation requires more operations per time step, both of which are undesirable.

### 6.1.1 Varying Time Step

One modification to discrete curve untangling process is to **vary the time step**. Instead of using a fixed time step  $\Delta T > 0$ , one could try modified backtracking Armijo line search[1] as described in Algorithm 6.1. (For simplicity, Algorithm 6.1 is expressed for explicit Euler scheme.) Note that time step  $\Delta T^k$  decreases only when needed, hence avoids self-crossing; this gives collision avoidance guarantee<sup>9</sup> by construction[12]. However, this requires an algorithm for detecting the change in the isotopy class of the curve.

---

<sup>9</sup>At least in terms of discretised curve.

### 6.1.2 Varying the Sample Points

Another modification of the discrete curve untangling process is to **vary the sample points**. When some of the edges of the discrete curve grow disproportionately large compared to most edges, this can render the TPE quadrature unusable. An alternative to adding a constraint energy to fix edge lengths is to resampling points around troublesome edges. One uses the points around the growing edges to approximate the portion of the curve by a spline. The advantage of this method is that it results in flexibility to change the resolution of the curve sensibly at any time during evolution, at the cost of potential errors which could lead to self-crossing if not careful.

### 6.1.3 Discussion of Fractional Sobolev Space

While this dissertation focused on  $L^2$  and  $H^1$  gradient flow for the untangling process, for given  $\alpha$  and  $\beta$  values for the TPE, there is an optimal choice of space for one to implement the curve untangling process, which makes the evolution by (5.13) the fastest and its computation trivial. It turns out that one could choose the gradient flow over **fractional Sobolev space**  $H^s$  where  $s = \frac{\beta-1}{\alpha}$  to achieve this[12]. Just as fractional derivative operators on  $\mathbb{R}$  are non-local, the gradient operator  $\text{grad}_{H^s} \mathcal{E}_\beta^\alpha(\Gamma^k)$  over the generalised Sobolev space  $H^s$  is also nonlocal. This gradient operator relies on the definition of fractional Laplacian[5]: for  $s \in (0, 1)$ ,

$$(-\Delta)^s u(\mathbf{x}) = C_{n,s} \int_{\mathbb{R}^n} \frac{u(\mathbf{x}) - u(\mathbf{y})}{|\mathbf{x} - \mathbf{y}|^{n+2s}} dV_y \quad (6.1)$$

$$= -\frac{1}{2} C_{n,s} \int_{\mathbb{R}^n} \frac{u(\mathbf{x} + \mathbf{y}) + u(\mathbf{x} - \mathbf{y}) - 2u(\mathbf{x})}{|\mathbf{y}|^{n+2s}} dV_y \quad (6.2)$$

$$= \mathcal{F}^{-1}(|\xi|^{2s} (\mathcal{F}u)) \quad (6.3)$$

where  $\mathcal{F}$  is the Fourier transform operator,  $f$  is the principal value integral as in the definition of inverse Fourier transform, and  $C_{n,s}$  is some constant that makes the last equality valid. It is sensible to attempt nonlocal gradient operator, as the TPE itself is, in some sense, nonlocal. For more detail, see [5], and [12] for its adaptation to curve repulsion.

## 6.2 An Alternative Approach via Approximation Theory

Motivated by the fact that we have approximated a curve by discretisation, and the TPE is “continuous” in the sense that small perturbation leads to small change, one could attempt untangling problem with a different framework. Instead of solving a discretised gradient flow equation (5.13), one could use approximation theory; if one knows beforehand that the initial curve is homeomorphic to a circle or a line segment, it is possible to interpret and approximate the curve as comprised of simple functions, and significantly optimise the untangling process by casting the functional

reduction problem to a traditional function reduction problem. This also results in a *simpler implementation* for low-stake/intensity applications, such as rope physics for video games. Denote by  $\mathbb{S}$  and  $\mathbb{L}$  for bounded curves that are homeomorphic to a circle and a line segment, respectively, as in Appendix C.

### 6.2.1 Curves in $\mathbb{S}$

For a continuous  $2\pi$ -periodic 1D function  $f : \mathbb{R} \rightarrow \mathbb{R}$  (where one only needs to define  $f$  on  $[0, 2\pi]$ ), there exists a Fourier series representation:

$$f(x) = \frac{a_0}{2} + \sum_{n=1}^{\infty} (a_n \cos(nx) + b_n \sin(nx)) \quad (6.4)$$

$$= \sum_{n=-\infty}^{\infty} c_n e^{inx} \quad (6.5)$$

where the two representations are equivalent. The coefficients are given by

$$a_n = \frac{1}{\pi} \int_0^{2\pi} f(x) \cos(nx) dx \in \mathbb{R} \quad (6.6)$$

$$b_n = \frac{1}{\pi} \int_0^{2\pi} f(x) \sin(nx) dx \in \mathbb{R} \quad (6.7)$$

$$c_n = \frac{1}{2\pi} \int_0^{2\pi} f(x) e^{-inx} dx \in \mathbb{C} \quad (6.8)$$

Now, for a vector-valued function such as a parameterised curve  $\gamma : \mathbb{R} \rightarrow \mathbb{R}^3$ , one could write 3D Fourier series, one for each coordinate (Figure 6.2):

$$\gamma(t) = \frac{1}{2} \begin{pmatrix} a_{1,0} \\ a_{2,0} \\ a_{3,0} \end{pmatrix} + \sum_{n=1}^{\infty} \begin{pmatrix} a_{1,n} & b_{1,n} \\ a_{2,n} & b_{2,n} \\ a_{3,n} & b_{3,n} \end{pmatrix} \begin{pmatrix} \cos(nt) \\ \sin(nt) \end{pmatrix} \quad (6.9)$$

$$= \sum_{n=-\infty}^{\infty} \begin{pmatrix} c_{1,n} \\ c_{2,n} \\ c_{3,n} \end{pmatrix} e^{int} \quad (6.10)$$

where the coefficients  $\{a_{i,n}\}, \{b_{i,n}\}, \{c_{i,n}\}$  are given by

$$a_{i,n} = \frac{1}{\pi} \int_0^{2\pi} \gamma_i(t) \cos(nt) dt \in \mathbb{R} \quad (6.11)$$

$$b_{i,n} = \frac{1}{\pi} \int_0^{2\pi} \gamma_i(t) \sin(nt) dt \in \mathbb{R} \quad (6.12)$$

$$c_{i,n} = \frac{1}{2\pi} \int_0^{2\pi} \gamma_i(t) e^{-int} dt \in \mathbb{C} \quad (6.13)$$

for  $i = 1, 2, 3$  where  $\gamma_i$  represents  $i^{\text{th}}$  coordinate of  $\gamma$ .

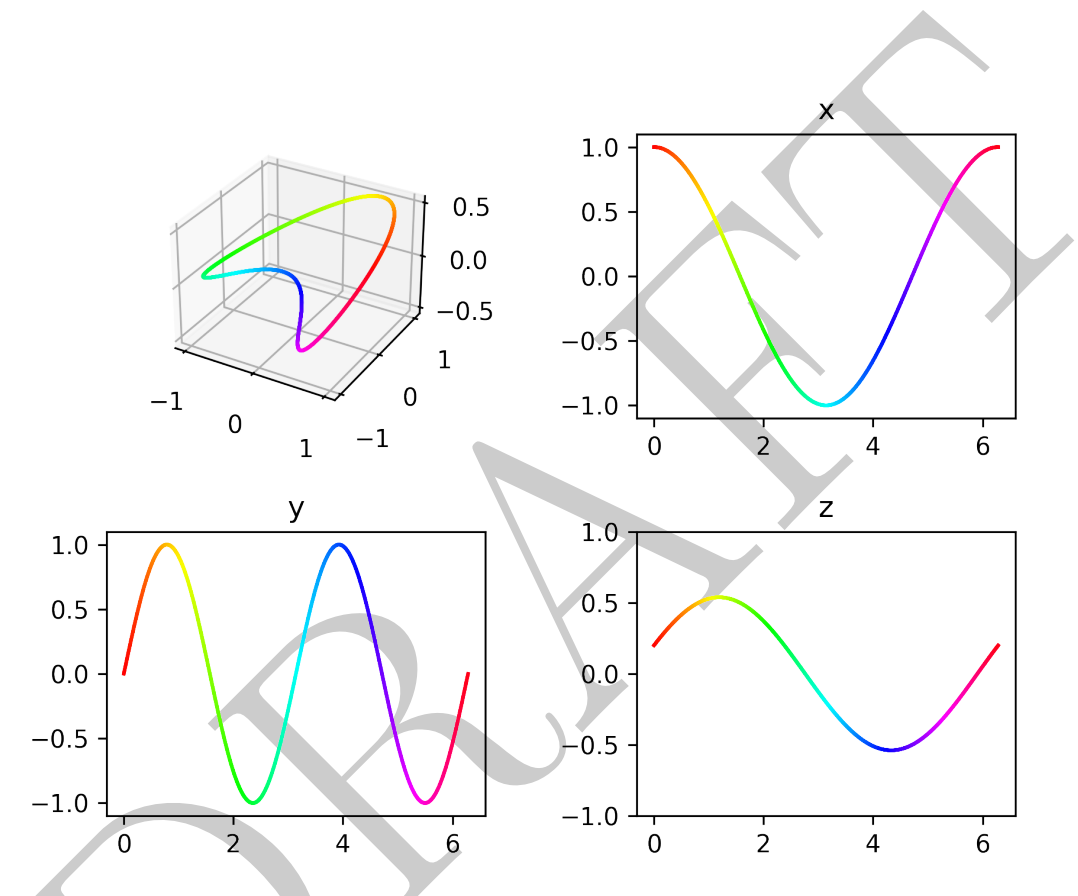


Figure 6.2: Decomposition of curve  $\gamma \in \mathbb{S}$  into 1D functions in each coordinate.

Now the idea is to truncate the series to order  $J > 0$  terms and collect its coefficients, that is,

$$\gamma(t) \approx \sum_{n=-J}^J \underbrace{\begin{pmatrix} c_{1,n} \\ c_{2,n} \\ c_{3,n} \end{pmatrix}}_{\mathbf{c}_n} e^{int}$$

One may justify the truncation of Fourier series representation by the following remark:

*Remark* (Rate of Convergence for Fourier Series[8]). For sufficiently well-behaving  $f \in \mathcal{C}^{p-1}$ , typically the nonzero coefficients  $c_n$  decay as  $O\left(\frac{1}{n^{p+1}}\right)$ . This can be made more rigorous by theorem 6.1, and the remark following it.

Now, using these coefficients, one could construct the approximate discrete curve  $\Gamma_{N,J}$  of resolution  $N \gg J$ . Take the dependent variables for the TPE to be the coefficients on Fourier series representation:

$$\mathcal{E}_\beta^\alpha(\gamma) \approx \mathcal{E}_\beta^\alpha(\gamma_J) = \mathcal{E}_\beta^\alpha(\underbrace{\mathbf{c}_{-J}, \mathbf{c}_{-J+1}, \dots, \mathbf{c}_J}_{3(2J+1) \text{ variables}}) \approx E_\beta^\alpha(\Gamma_{N,J}) \quad (6.14)$$

This time, instead of solving for gradient flow equation, we use standard methods of minimising a function, such as gradient descent or otherwise *over the  $3(2J + 1)$  coefficients*<sup>10</sup>  $\mathbf{c}_{-J}, \mathbf{c}_{-J+1}, \dots, \mathbf{c}_J$ . It is practical to take  $N$  to be larger than the resolution for the discrete gradient flow, as we will have less variables to minimise over. The smoothness of the evolving curve follows since it is represented as a finite sum of infinitely smooth function, so there is no misbehaviour from sharp points as in Figure 5.3.

### 6.2.2 Curves in $\mathbb{L}$

For  $\gamma$  that is not closed, but rather homeomorphic to a line segment, it is more natural to use Chebyshev approximation[11].

**Definition** (Chebyshev Polynomial).  $n^{\text{th}}$  Chebyshev polynomial  $T_n(x)$  over  $[-1, 1]$  is defined in the following way:

$$x = \frac{1}{2} (z + z^{-1}) = \cos \theta \quad (6.15)$$

$$T_n(x) = \frac{1}{2} (z^n + z^{-n}) = \cos(n\theta) \quad (6.16)$$

where  $z \in \{z \in \mathbb{C} \mid |z| = 1\}$ .

---

<sup>10</sup>Without loss of generality, one could take  $c_{i,0} = 0$  for  $i = 1, 2, 3$  as it only determines constant shift of the entire curve, so one actually only needs to consider  $6J$  coefficients.

For a curve  $\gamma : [-1, 1] \rightarrow \mathbb{R}^3$  such that  $\gamma \in \mathbb{L}$ , there exists a Chebyshev series representation:

$$\gamma(t) = \underbrace{\begin{pmatrix} a_{1,0} \\ a_{2,0} \\ a_{3,0} \end{pmatrix}}_{\mathbf{a}_0} + \sum_{n=1}^{\infty} \underbrace{\begin{pmatrix} a_{1,n} \\ a_{2,n} \\ a_{3,n} \end{pmatrix}}_{\mathbf{a}_n} T_n(t) \quad (6.17)$$

where  $T_n(t)$  is the  $n^{\text{th}}$  Chebyshev polynomial. The coefficients  $\{a_{i,n}\}$  are given by:

$$a_{i,n} = \frac{2}{\pi} \int_{-1}^1 \frac{\gamma_i(t) T_n(t)}{\sqrt{1-t^2}} dt \quad (6.18)$$

for  $i = 1, 2, 3$ .

We again approximate  $\gamma$  by truncating the Chebyshev series up to order  $J$  term, which we justify by the following theorem for Chebyshev series:

**Theorem 6.1** (Rate of Convergence for Chebyshev Series[11]). *For  $f : [-1, 1] \rightarrow \mathbb{R}$  such that its derivatives through  $f^{(p-1)}$  are absolutely continuous, and  $f^{(p)}$  is of bounded variation, then the nonzero coefficients decay as  $O\left(\frac{1}{n^{p+1}}\right)$  and the 2-norm error of interpolants and truncations decay as  $O\left(\frac{1}{n^p}\right)$ .*

*Remark.* There is actually a way in a sense that Chebyshev series and Fourier series are equivalent, which is outlined in [11]. The remark of rate of convergence of Fourier series can be posed, hence, equivalently to this theorem.

Then, interpret the TPE as a function of the coefficients of the series.

$$\mathcal{E}_{\beta}^{\alpha}(\gamma) \approx \mathcal{E}_{\beta}^{\alpha}(\gamma_J) = \mathcal{E}_{\beta}^{\alpha} \underbrace{(\mathbf{a}_0, \mathbf{a}_1, \dots, \mathbf{a}_J)}_{3(J+1) \text{ variables}} \approx E_{\beta}^{\alpha}(\boldsymbol{\Gamma}_{N,J}) \quad (6.19)$$

This time, the TPE quadrature is taken as the one in Appendix C.1.

### 6.2.3 Sample Points and Time Complexity

While approximation via series reduces the number of dimensions to reduce the TPE over, in order to compute the derivative (against coefficients), one still needs to use quadrature, meaning, one needs to take  $N$  sample points.

Because we have captured the function defining the curve rather than points, there is more flexibility to either sample/resample points as needed, simply by varying the parameters for the sample points.

There are natural choice of sample points for curves in  $\mathbb{S}$  and  $\mathbb{L}$ .

- For a curve  $\gamma \in \mathbb{S}$ , the natural sample points are points of which the parameter values are equispaced on the interval  $[0, 2\pi]$ .

$$\left\{ \gamma(t) \middle| t = \frac{2\pi}{N}j, j \in \{0, 1, \dots, N-1\} \right\} \quad (6.20)$$

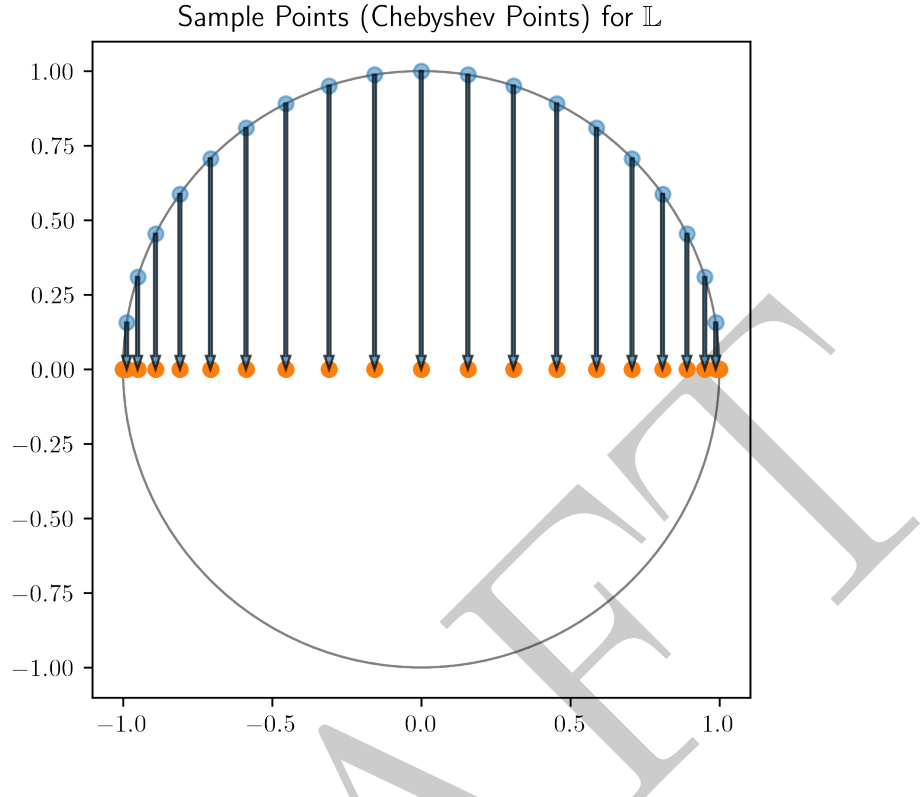


Figure 6.3: Chebyshev points are acquired from projecting equally spaced points on a unit circle to the  $x$ -axis. Note that the “density” of points is the highest at the ends.

- For a curve  $\gamma \in \mathbb{L}$ , the natural choice of sample points are Chebyshev points on the interval. (Figure 6.3)

$$\left\{ \gamma(t) \mid t = \cos\left(\frac{j\pi}{N}\right), j \in \{0, 1, \dots, N\} \right\} \quad (6.21)$$

Use of Chebyshev points may aid in avoiding Runge phenomenon<sup>11</sup>[11].

Note that keeping  $N$  constant during evolution allows one to optimise the generation/computation of sample points. For example, for  $\gamma \in \mathbb{S}$ , the points on the discretised curve  $\Gamma_{N,J}^k$ :

$$\Gamma_{N,J}^k[j] = \mathbf{x}_j^k = \sum_{n=-J}^J \mathbf{c}_n e^{i \frac{2\pi}{N} nj} \quad j = 0, 1, \dots, N-1 \quad (6.22)$$

By using modified FFT[3], one could reduce the cost from  $O(NJ)$  to  $O(J \log N)$ . Also, because the TPE of the truncated curve  $\mathcal{E}_\beta^\alpha(\gamma_J)$  involves integral which the

---

<sup>11</sup>Exponential divergence at the boundary; an example of instability in interpolation.

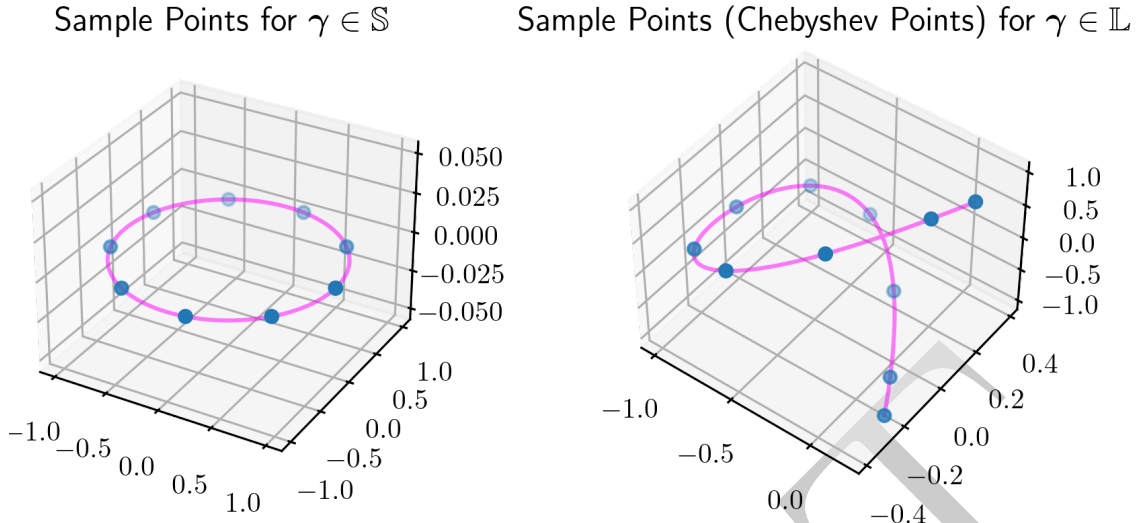


Figure 6.4: Natural sample points on  $\gamma \in \mathbb{S}$  and  $\gamma \in \mathbb{L}$

integration variable is independent from the coefficients  $c_n$ , one could, in theory, directly compute derivative by differentiating under the integral sign (which turns out to be a messy computation, but possible), or one could use central difference scheme to approximate it; because one only needs to compute  $3J$  derivatives<sup>12</sup> instead of  $3N \gg 3J$  derivatives, this can be a practical approach. With latter approach to compute derivative, this would result in  $O(J^3 + J \log N)$  operations per time step. Because  $J$  does not need to be large at all<sup>13</sup>, and in fact, assuming sufficiently fast decay of higher order coefficients, one could “deflate” the problem by truncating the series further later, the “practical cost” (assuming  $J$  is of constant order) is  $O(\log N)$  with this approach.

Similar analysis can be done with curves in  $\mathbb{L}$  as the evaluation of Chebyshev series can also be improved using FFT[11].

The full algorithm with deflation is outlined in Algorithm 6.2. As demonstrated in Figure 6.6, this method can indeed be practical.

### 6.3 Potential Extension: Ribbon-like Objects

The dissertation explored a few methods of untangling a curve. In practice, however, we face untangling problem with ribbon-like objects as well, which hold additional properties such as intrinsic curvatures, surface tension, and elasticity.

One could model this as a membrane  $\Sigma$  and consider additional energy such as

<sup>12</sup>Order 0 terms do not contribute as TPE is shift-invariant, hence derivative with respect to those coefficients are identically zero.

<sup>13</sup>Instead of capturing a unit circle with, say  $N = 90$  points, one technically only needs  $J = 1$  to do the same.

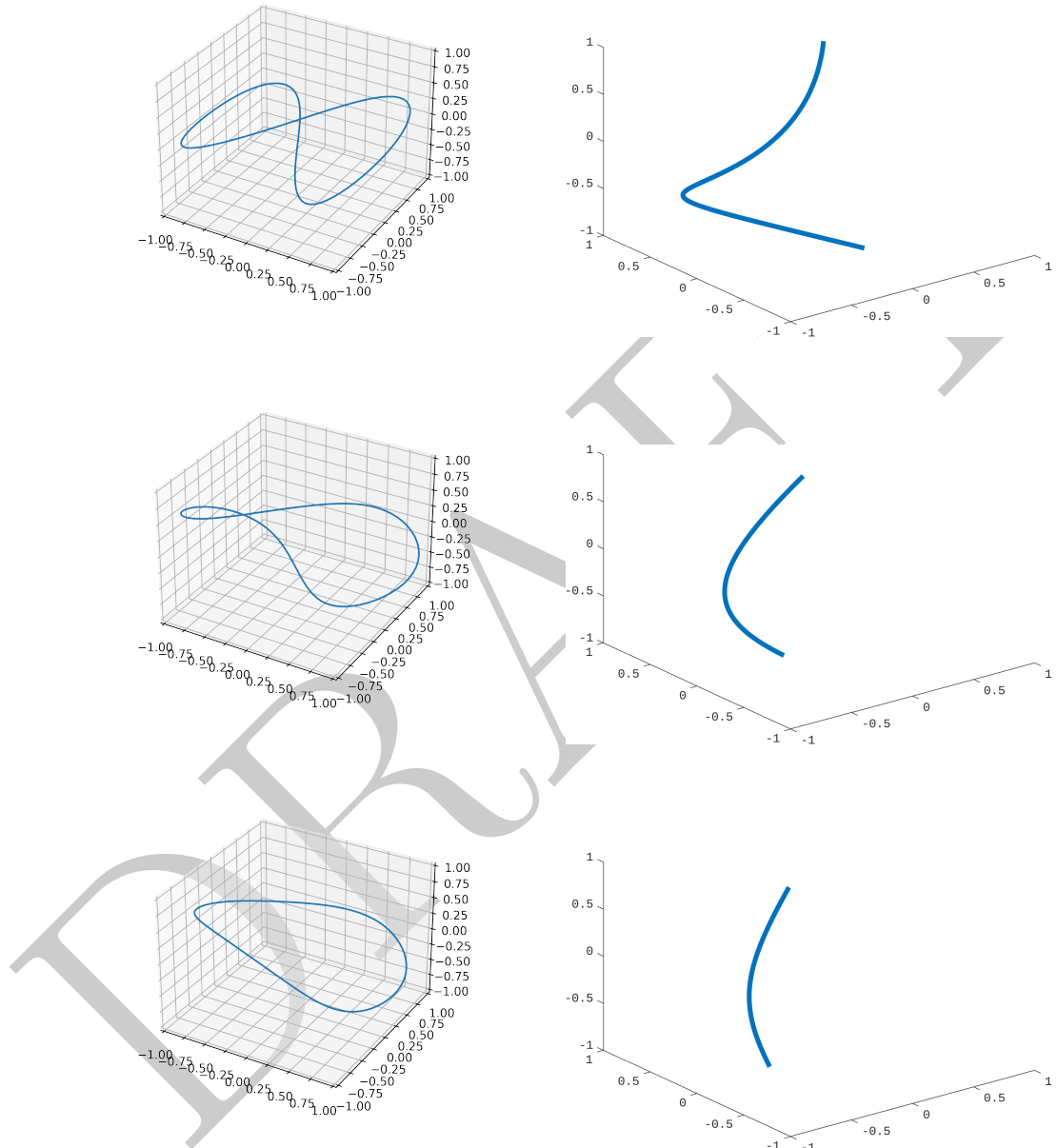


Figure 6.5: Evolution of  $\gamma \in \mathbb{S}$  and  $\gamma \in \mathbb{L}$ .

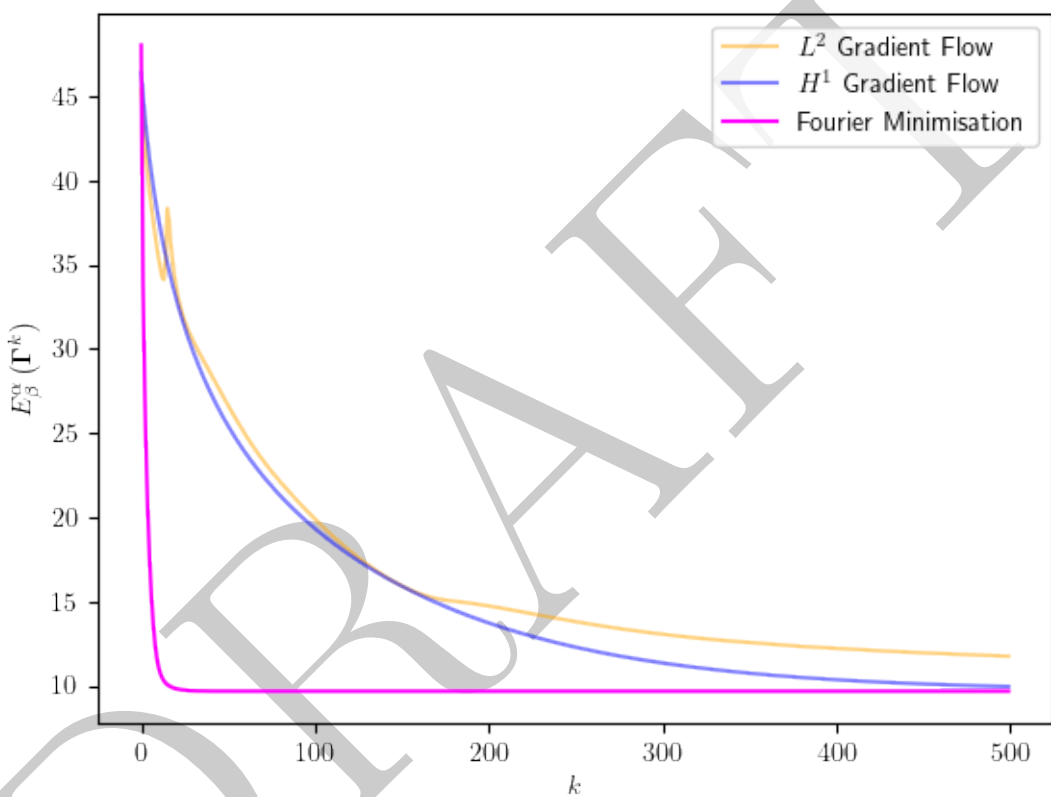


Figure 6.6: The method of minimising function can be much faster than using the gradient flow.

---

**Algorithm 6.2** Fixed Step-size Energy Reduction via Approximation Theory with Deflation

---

Choose  $J$ . (Depends on the complexity of the initial curve.)  
 Let  $k = 0$ .  
 Choose  $M > 0$ , the number of time steps.  
 Choose  $N > J$ , the resolution of the curve to generate.  
 Choose  $0 < \epsilon \ll 1$ , the tolerance for deflation.  
 Choose  $0 < \Delta T \ll 1$ , the fixed step size.  
 Given initial curve  $\gamma$  or initial set of sample points  $\Gamma$ , find a series approximation up to order  $J$ .

**while**  $k < M$  **do**

- Compute sample points  $\Gamma_{N,J}^k$  as in (6.22) via FFT.
- Compute  $\nabla_c E_\beta^\alpha(\Gamma_{N,J}^k)$  exactly or approximately, where the  $\nabla_c$  is gradient operator over all the coefficients of the series.  $\triangleright c$  is the array of coefficients.
- Evolve a time step by  $c \leftarrow c - \Delta T \nabla_c E_\beta^\alpha(\Gamma_{N,J}^k)$ .
- if**  $\exists j$  s.t.  $\forall i \geq j$ ,  $|c_i| < \epsilon$  **then**
- Truncate the series to order  $j - i$  term.
- $J \leftarrow j - i$ .  $\triangleright$  Deflation: reduced  $J$ , so expect a speedup in computation.
- end if**
- $k \leftarrow k + 1$

**end while**

---

following[7]:

$$\mathcal{E}_\Sigma := \iint_\Sigma (\gamma + 2\kappa(H - H_0)^2 + \bar{\kappa}K_g) dS \quad (6.23)$$

where

- $H$  and  $K_G$  are the mean and Gaussian curvatures respectively.
- $\gamma$  is the surface tension.
- $\kappa$  and  $\bar{\kappa}$  are the bending and saddle-splay modulus respectively.
- $H_0$  is the intrinsic mean curvature.

While formal definitions of the terms are out of scope of this dissertation, by reducing  $\tilde{\mathcal{E}}_\beta^\alpha + \mathcal{E}_\Sigma + \mathcal{C}$  where  $\tilde{\mathcal{E}}_\beta^\alpha = \iint_\Sigma \iint_\Sigma \tilde{k} dS dS'$  is generalised TPE for membranes, one could easily conceive a numerical scheme for untangling, for example, DNA strands (Figure 6.7) and by extension, tackling surface optimisation problems.

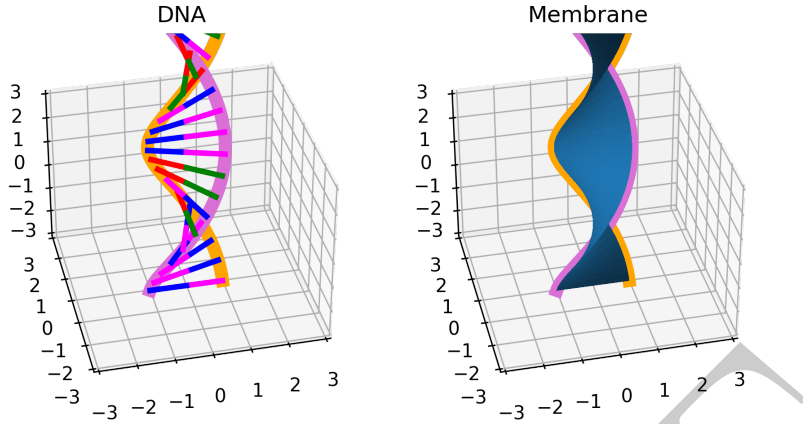


Figure 6.7: DNA is a ribbon-like structure which is often found wound around histone protein.[6]

# Appendices

## A Definitions of Important Inner Product Spaces

(Based on definitions from [10]. We focus our attention to interval  $I \subset \mathbb{R}$ .) Here are some of the notable inner product spaces.

### A.1 $L^2$ Space

**Definition ( $L^2$  Space).** For interval  $I \subset \mathbb{R}$ ,  $L^2$  space over is defined as

$$L^2 = \left\{ f : I \rightarrow \mathbb{R} \mid f \text{ measurable}, \left( \int_I |f|^2 dx \right)^{1/2} < \infty \right\} \quad (\text{A.1})$$

$L^2$  inner product is defined as

$$\forall f, g \in L^2 \quad \langle f, g \rangle_{L^2} = \int_I fg dx \quad (\text{A.2})$$

### A.2 $H^k$ Space

To define Sobolev (inner product) spaces (denoted  $H^k$  where  $k \in \mathbb{N} \cup \{0\}$ ) one must define weak derivative operator  $D$ :

**Definition (Weak Derivative).** For  $u$  locally integrable on  $I$ , if there exists  $w$  such that for all infinitely smooth  $v : I \rightarrow \mathbb{R}$  with compact support,

$$\int_I wv dx = (-1)^\alpha \int_I u \frac{d^\alpha v}{dx^\alpha} dx \quad (\text{A.3})$$

then  $w$  is said to be **weak derivative** of order  $\alpha$  of  $u$ , and one writes  $D^\alpha u = w$ .

Weak derivative extends the definition of conventional derivative, and is equivalent to the conventional derivative for smooth functions. With weak derivatives introduced, one may now define Sobolev inner product spaces.

**Definition ( $H^k$  Space).** Sobolev inner product space of order  $k \in \mathbb{N} \cup \{0\}$  (denoted  $H^k$ ) is defined as

$$H^k = \left\{ f \in L^2 \mid D^\alpha f \in L^2, \alpha \leq k \right\} \quad (\text{A.4})$$

$H^k$  inner product is defined as:

$$\forall f, g \in H^k \quad \langle f, g \rangle_{H^2} = \sum_{\alpha \leq k} \langle D^\alpha f, D^\alpha g \rangle_{L^2} \quad (\text{A.5})$$

*Remark.* Note that  $H^0 = L^2$  by definition. One could say that Sobolev inner product spaces extend  $L^2$  space. It also turns out that  $H^k$  are Hilbert spaces.

## B Gradient Operator in Sobolev Spaces

For acquiring gradient on integer Sobolev spaces from  $L^2$  gradient over boundary-free  $\Omega$ , there are two main “rules” one could use.

**Lemma B.1** (Shifting Gradient Operator).

$$\langle \nabla f, \nabla g \rangle_{L^2} = -\langle \Delta f, g \rangle_{L^2} = -\langle f, \Delta g \rangle_{L^2} \quad (\text{B.1})$$

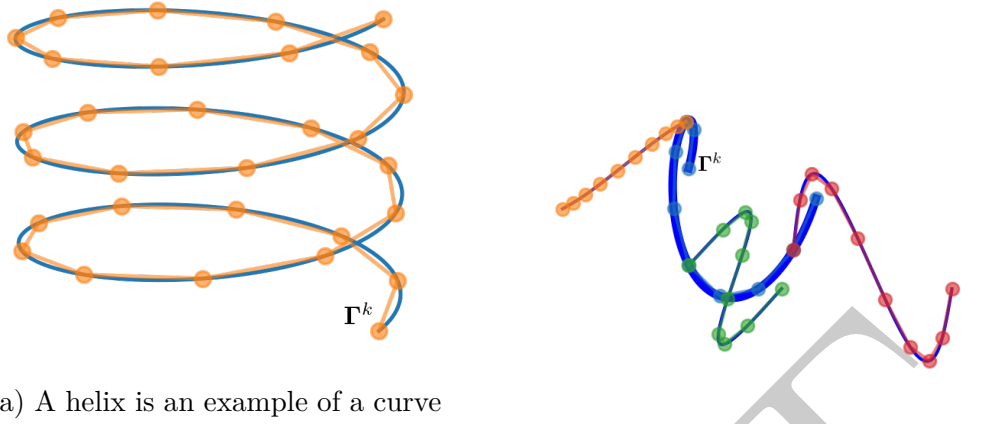
*Proof.*

$$\begin{aligned} \langle \nabla f, \nabla g \rangle_{L^2} &= \int_{\Omega} \nabla f \cdot \nabla g \, dV \\ &= \int_{\Omega} (\nabla \cdot (g \nabla f) - g \Delta f) \, dV \\ &\stackrel{\text{IBP}}{=} \underbrace{\oint_{\partial\Omega} g \nabla f \cdot \mathbf{n} \, ds}_{\text{Boundary Term}} - \int_{\Omega} g \Delta f \, dV \\ &= -\langle \Delta f, g \rangle_{L^2} + \underbrace{\oint_{\partial\Omega} g \nabla f \cdot \mathbf{n} \, ds}_{\text{Boundary Term}} \end{aligned}$$

For boundary-free  $\Omega$ , boundary terms can be taken to be zero. ■

**Lemma B.2** (Shifting Laplacian Operator).

$$\langle \Delta f, g \rangle_{L^2} = \langle f, \Delta g \rangle \quad (\text{B.2})$$



(a) A helix is an example of a curve homeomorphic to a line segment, so is in  $\mathbb{L}$ . Another notable curve in this class is a trefoil.

(b) A curve with 3 branches from a main “stem”. This curve is homeomorphic to some tree, so is in  $\overline{\mathbb{L}}$ .

Figure C.1: Curves in different homeomorphism classes.

*Proof.*

$$\begin{aligned}
 \langle \Delta f, g \rangle_{L^2} &= \int_{\Omega} g \Delta f \, dV \\
 &= \int_{\Omega} (\nabla \cdot (g \nabla f) - \nabla f \cdot \nabla g) \, dV \\
 &\stackrel{\text{IBP}}{=} \underbrace{\int_{\partial\Omega} g \nabla f \cdot \mathbf{n} \, ds}_{\text{Boundary Term}} - \int_{\Omega} \nabla f \cdot \nabla g \, dV \\
 &= \underbrace{\int_{\partial\Omega} g \nabla f \cdot \mathbf{n} \, ds}_{\text{Boundary Term}} - \langle \nabla f, \nabla g \rangle_{L^2}
 \end{aligned}$$

Now, use lemma B.1 and take boundary terms to be zero. ■

## C Tangent-Point Energy Quadrature: Other Homeomorphism Classes

Because homeomorphism relation is an equivalence relation, one could define equivalence classes. We will call them homeomorphism classes. *We restrict our discussion to bounded curves.*

To make notation more concise, we introduce some labels:

- Write  $\mathbb{S}$  for the equivalence class of curves that are simple and closed; in other words, curves homeomorphic to a unit circle.
- Write  $\mathbb{L}$  for the equivalence class of curves that are homeomorphic to a line segment.

- Write  $\bar{\mathbb{L}}$  for the union of equivalence classes for curves that are homeomorphic to a tree graph, or a “bus network”.

We have defined tangent-point energy quadrature for  $\gamma \in \mathbb{S}$  at (5.7).

For curves in different homeomorphism classes, one may make minor changes to (5.7) to get a sensible quadrature.

Note that because curves in  $\mathbb{L}$  and  $\bar{\mathbb{L}}$  may have boundaries unlike curves in  $\mathbb{S}$ . For the gradient operators derived in section 2.2.1 to be applicable, one assumes natural boundary conditions; where the boundary integrals in lemma B.1 and B.2 to be zero for any  $g$  appropriate.

## C.1 Curves in $\mathbb{L}$

Given a curve  $\gamma \in \mathbb{L}$  such as the helix (Figure C.1(a)), one could take the following as its tangent-point energy quadrature for its discretisation  $\Gamma^k$ :

$$E_\beta^\alpha(\Gamma^k) := \sum_{\substack{i,j \in \{1, \dots, N-2\} \\ r(i-j,N) > 1}} K_\beta^\alpha(i,j) |e_i| |e_j| \quad (\text{C.1})$$

where the contribution from each end is neglected. Note that unlike a curve from  $\mathbb{S}$  one need not generalise the indexing rule to be “cyclic”.

## C.2 Curves in $\bar{\mathbb{L}}$

For a curve  $\gamma \in \bar{\mathbb{L}}$  that has  $m$  “branches” from a single “stem”, one needs to take into account of at what points on the discretisation branching happens. Suppose for all branches protrude from the stem. On Figure C.1(b), the stem is represented by the thick blue curve.

One can capture this curve by an array of the following form.

$$\Gamma^k = \left( \underbrace{\mathbf{x}_{0,0}^k, \dots, \mathbf{x}_{0,n_0-1}^k}_{\text{Stem}} \middle| \underbrace{\mathbf{x}_{1,0}^k, \dots, \mathbf{x}_{1,n_1-1}^k}_{\text{Branch 1}} \middle| \dots \middle| \underbrace{\mathbf{x}_{m,0}^k, \dots, \mathbf{x}_{m,n_m-1}^k}_{\text{Branch } m} \right) \quad (\text{C.2})$$

where the “linkage points” for branches to the stem are  $\mathbf{x}_{1,0}^k, \dots, \mathbf{x}_{m,0}^k$ , which can be identified by the fact that  $\mathbf{x}_{1,0}^k, \dots, \mathbf{x}_{m,0}^k \in \{\mathbf{x}_{0,0}^k, \dots, \mathbf{x}_{0,n_0-1}^k\}$ , that is, all duplicate points are to be understood as linkage points. Denote the multiset<sup>14</sup> of linkage points as  $L(\Gamma^k)$ . Then one may note the relation  $N = \sum_{i=0}^m n_i - |L(\Gamma^k)| = \sum_{i=0}^m n_i - m$ . Note that this is a natural generalisation for curves in  $\bar{\mathbb{L}}$ .

Now, one may write a tangent-point energy quadrature as:

$$E_\beta^\alpha(\Gamma^k) := \sum_{p,q \in \{0,1,\dots,m\}} \sum_{\substack{i \in \{1,\dots,n_p-2\} \\ j \in \{1,\dots,n_q-2\} \\ \sigma(e_{p,i}, e_{q,j})=1}} K_\beta^\alpha(p_i, q_j) |e_{p,i}| |e_{q,j}| \quad (\text{C.3})$$

---

<sup>14</sup>“a set that allows multiplicity of same elements”

where  $p_i$  (similarly with  $q_j$ ) refers to the index of vector  $\mathbf{x}_{p,i}^k$  in (C.2), that is,

$$p_i = \sum_{j=0}^{p-1} n_j + i$$

and

$$\sigma(e_1, e_2) = \begin{cases} 0 & \exists \text{ shared vertex between edges } e_1, e_2 \\ 1 & \text{Otherwise} \end{cases}$$

*Remark.* Representation (C.2) is **not unique**; for example, one could take different curve to be the “stem”. The quadrature (C.3) is, however, invariant under different representation, hence well-defined.

## D Exact $\ell^2$ Gradient of $E_\beta^\alpha$

Recall the discretisation of tangent-point energy for simple closed curve  $\Gamma^k$  from (5.7) with  $K_\beta^\alpha$  defined by (5.6).

To compute  $\text{Grad}_{\ell^2} E_\beta^\alpha(\Gamma^k)$ , one can consider subproblem of computing  $\nabla_{\mathbf{x}_k} E_\beta^\alpha(\Gamma)$  for each  $k = 0, 1, \dots, N-1$ .

Fix  $k$ . The  $4(N-3)$  pairs of indices  $(i, j)$  where the summand  $K_\beta^\alpha(i, j) |\mathbf{e}_i| |\mathbf{e}_j|$  involves  $\mathbf{x}_k$  are:

- $(k, 0), \dots, (k, k-2), (k, k+2), \dots, (k, N-1)$
- $(k-1, 0), \dots, (k-1, k-3), (k-1, k+1), \dots, (k-1, N-1)$
- $(0, k), \dots, (k-2, k), (k+2, k), \dots, (N-1, k)$
- $(0, k-1), \dots, (k-3, k-1), (k+1, k-1), \dots, (N-1, k-1)$

We now attempt to construct explicit derivative in a “modular fashion”. If we take gradient of the summand directly,<sup>15</sup>

$$\nabla_{\mathbf{x}_k} (K_\beta^\alpha(i, j) |\mathbf{e}_i| |\mathbf{e}_j|) = |\mathbf{e}_i| |\mathbf{x}_j| \nabla_{\mathbf{x}_k} K_\beta^\alpha(i, j) + K_\beta^\alpha(i, j) \nabla_{\mathbf{x}_k} (|\mathbf{e}_i| |\mathbf{e}_j|) \quad (\text{D.1})$$

Due to restriction  $r(i-j, N) > 1$ , at most one of  $|\mathbf{e}_i|$  and  $|\mathbf{x}_j|$  may involve  $\mathbf{x}_k$  at a time.

First note that, if  $m \neq k$ ,

$$\nabla_{\mathbf{x}_k} |\mathbf{x}_k - \mathbf{x}_m| = \frac{\mathbf{x}_k - \mathbf{x}_m}{|\mathbf{x}_k - \mathbf{x}_m|} \quad (\text{D.2})$$

---

<sup>15</sup>recall  $|\mathbf{e}_i| = |\mathbf{x}_i - \mathbf{x}_{i+1}|$  and  $|\mathbf{e}_j| = |\mathbf{x}_j - \mathbf{x}_{j+1}|$ .

Now, the demanding part is to compute  $\nabla_{\mathbf{x}_k} k_\beta^\alpha$ , since it is needed for computing  $\nabla_{\mathbf{x}_k} K_\beta^\alpha$ . Note that

$$\begin{aligned} k_\beta^\alpha(\mathbf{x}_p, \mathbf{x}_q, \mathbf{T}_r) &= k_\beta^\alpha \left( \mathbf{x}_p, \mathbf{x}_q, \frac{\mathbf{x}_{r+1} - \mathbf{x}_r}{|\mathbf{x}_{r+1} - \mathbf{x}_r|} \right) \\ &= \frac{\sqrt{|\mathbf{x}_{r+1} - \mathbf{x}_r|^2 |\mathbf{x}_p - \mathbf{x}_q|^2 - ((\mathbf{x}_{r+1} - \mathbf{x}_r) \cdot (\mathbf{x}_p - \mathbf{x}_q))^2}}{|\mathbf{x}_p - \mathbf{x}_q|^\beta |\mathbf{x}_{r+1} - \mathbf{x}_r|^\alpha} \\ &= \frac{(\xi_{p,q,r})^{\alpha/2}}{\eta_{p,q,r}} \end{aligned} \quad (\text{D.3})$$

where we have defined

$$\begin{aligned} \xi_{p,q,r} &:= |\mathbf{x}_{r+1} - \mathbf{x}_r|^2 |\mathbf{x}_p - \mathbf{x}_q|^2 - ((\mathbf{x}_{r+1} - \mathbf{x}_r) \cdot (\mathbf{x}_p - \mathbf{x}_q))^2 \\ \eta_{p,q,r} &:= |\mathbf{x}_p - \mathbf{x}_q|^\beta |\mathbf{x}_{r+1} - \mathbf{x}_r|^\alpha \end{aligned}$$

Then, we may express  $\nabla_{\mathbf{x}_k} k_\beta^\alpha(\mathbf{x}_p, \mathbf{x}_q, \mathbf{T}_r)$  as:

$$\begin{aligned} \nabla_{\mathbf{x}_k} k_\beta^\alpha(\mathbf{x}_p, \mathbf{x}_q, \mathbf{T}_r) &= \nabla_{\mathbf{x}_k} \left( \frac{(\xi_{p,q,r})^{\alpha/2}}{\eta_{p,q,r}} \right) \\ &= \frac{1}{(\eta_{p,q,r})^2} \left( \frac{\alpha}{2} (\xi_{p,q,r})^{\alpha/2-1} \eta_{p,q,r} \nabla_{\mathbf{x}_k} \xi_{p,q,r} - (\xi_{p,q,r})^{\alpha/2} \nabla_{\mathbf{x}_k} \eta_{p,q,r} \right) \end{aligned} \quad (\text{D.4})$$

It now remains to compute  $\nabla_{\mathbf{x}_k} \xi_{p,q,r}$  and  $\nabla_{\mathbf{x}_k} \eta_{p,q,r}$  for relevant  $(p, q, r)$  tuples.

There are five classes of relevant  $(p, q, r)$  tuples.

If  $(p, q, r) = (k, j, k)$ ,

$$\begin{aligned} \xi_{k,j,k} &= |\mathbf{x}_{k+1} - \mathbf{x}_k|^2 |\mathbf{x}_k - \mathbf{x}_j|^2 - ((\mathbf{x}_{k+1} - \mathbf{x}_k) \cdot (\mathbf{x}_k - \mathbf{x}_j))^2 \\ \eta_{k,j,k} &= |\mathbf{x}_k - \mathbf{x}_j|^\beta |\mathbf{x}_k - \mathbf{x}_{k+1}|^\alpha \\ \nabla_{\mathbf{x}_k} \xi_{k,j,k} &= 2(\mathbf{x}_k - \mathbf{x}_{k+1}) |\mathbf{x}_k - \mathbf{x}_j|^2 + 2|\mathbf{x}_{k+1} - \mathbf{x}_k|^2 (\mathbf{x}_k - \mathbf{x}_j) \\ &\quad - 2((\mathbf{x}_{k+1} - \mathbf{x}_k) \cdot (\mathbf{x}_k - \mathbf{x}_j)) (\mathbf{x}_j + \mathbf{x}_{k+1} - 2\mathbf{x}_k) \\ \nabla_{\mathbf{x}_k} \eta_{k,j,k} &= \beta |\mathbf{x}_k - \mathbf{x}_j|^{\beta-2} |\mathbf{x}_k - \mathbf{x}_{k+1}|^\alpha (\mathbf{x}_k - \mathbf{x}_j) \\ &\quad + \alpha |\mathbf{x}_k - \mathbf{x}_j|^\beta |\mathbf{x}_k - \mathbf{x}_{k+1}|^{\alpha-2} (\mathbf{x}_k - \mathbf{x}_{k+1}) \end{aligned}$$

If  $(p, q, r) = (i, j, k)$  where  $i \neq k$  and  $i \neq k-1$

$$\begin{aligned} \xi_{i,j,k} &= |\mathbf{x}_{k+1} - \mathbf{x}_k|^2 |\mathbf{x}_i - \mathbf{x}_j|^2 - ((\mathbf{x}_{k+1} - \mathbf{x}_k) \cdot (\mathbf{x}_i - \mathbf{x}_j))^2 \\ \eta_{i,j,k} &= |\mathbf{x}_i - \mathbf{x}_j|^\beta |\mathbf{x}_k - \mathbf{x}_{k+1}|^\alpha \\ \nabla_{\mathbf{x}_k} \xi_{i,j,k} &= 2|\mathbf{x}_i - \mathbf{x}_j|^2 (\mathbf{x}_k - \mathbf{x}_{k+1}) \\ &\quad - 2((\mathbf{x}_{k+1} - \mathbf{x}_k) \cdot (\mathbf{x}_i - \mathbf{x}_j)) (\mathbf{x}_j - \mathbf{x}_i) \\ \nabla_{\mathbf{x}_k} \eta_{i,j,k} &= \alpha |\mathbf{x}_i - \mathbf{x}_j|^\beta |\mathbf{x}_k - \mathbf{x}_{k+1}|^{\alpha-2} (\mathbf{x}_k - \mathbf{x}_{k+1}) \end{aligned}$$

If  $(p, q, r) = (k - 1, j, k - 1)$ ,

$$\begin{aligned}\xi_{k-1,j,k-1} &= |\mathbf{x}_k - \mathbf{x}_{k-1}|^2 |\mathbf{x}_{k-1} - \mathbf{x}_j|^2 - ((\mathbf{x}_k - \mathbf{x}_{k-1}) \cdot (\mathbf{x}_{k-1} - \mathbf{x}_j))^2 \\ \eta_{k-1,j,k-1} &= |\mathbf{x}_{k-1} - \mathbf{x}_j|^\beta |\mathbf{x}_{k-1} - \mathbf{x}_k|^\alpha \\ \nabla_{\mathbf{x}_k} \xi_{k-1,j,k-1} &= 2 |\mathbf{x}_{k-1} - \mathbf{x}_j|^2 (\mathbf{x}_k - \mathbf{x}_{k-1}) \\ &\quad - 2 ((\mathbf{x}_k - \mathbf{x}_{k-1}) \cdot (\mathbf{x}_{k-1} - \mathbf{x}_j)) (\mathbf{x}_{k-1} - \mathbf{x}_j) \\ \nabla_{\mathbf{x}_k} \eta_{k-1,j,k-1} &= \alpha |\mathbf{x}_{k-1} - \mathbf{x}_j|^\beta |\mathbf{x}_k - \mathbf{x}_{k-1}|^{\alpha-2} (\mathbf{x}_k - \mathbf{x}_{k-1})\end{aligned}$$

If  $(p, q, r) = (k, j, k - 1)$ ,

$$\begin{aligned}\xi_{k,j,k-1} &= |\mathbf{x}_k - \mathbf{x}_{k-1}|^2 |\mathbf{x}_k - \mathbf{x}_j|^2 - ((\mathbf{x}_k - \mathbf{x}_{k-1}) \cdot (\mathbf{x}_k - \mathbf{x}_j))^2 \\ \eta_{k,j,k-1} &= |\mathbf{x}_k - \mathbf{x}_j|^\beta |\mathbf{x}_{k-1} - \mathbf{x}_k|^\alpha \\ \nabla_{\mathbf{x}_k} \xi_{k,j,k-1} &= 2 |\mathbf{x}_k - \mathbf{x}_j|^2 (\mathbf{x}_k - \mathbf{x}_{k-1}) \\ &\quad + 2 |\mathbf{x}_k - \mathbf{x}_{k-1}|^2 (\mathbf{x}_k - \mathbf{x}_j) \\ &\quad - 2 ((\mathbf{x}_k - \mathbf{x}_{k-1}) \cdot (\mathbf{x}_k - \mathbf{x}_j)) (2\mathbf{x}_k - \mathbf{x}_j - \mathbf{x}_{k-1}) \\ \nabla_{\mathbf{x}_k} \eta_{k,j,k-1} &= \beta |\mathbf{x}_{k-1} - \mathbf{x}_k|^\alpha |\mathbf{x}_k - \mathbf{x}_j|^{\beta-2} (\mathbf{x}_k - \mathbf{x}_j) \\ &\quad + \alpha |\mathbf{x}_k - \mathbf{x}_j|^\beta |\mathbf{x}_k - \mathbf{x}_{k-1}|^{\alpha-2} (\mathbf{x}_k - \mathbf{x}_{k-1})\end{aligned}$$

If  $(p, q, r) = (i, k, j)$ ,

$$\begin{aligned}\xi_{i,k,j} &= |\mathbf{x}_{j+1} - \mathbf{x}_j|^2 |\mathbf{x}_k - \mathbf{x}_i|^2 - ((\mathbf{x}_{j+1} - \mathbf{x}_j) \cdot (\mathbf{x}_k - \mathbf{x}_i))^2 \\ \eta_{i,k,j} &= |\mathbf{x}_k - \mathbf{x}_i|^\beta |\mathbf{x}_j - \mathbf{x}_{j+1}|^\alpha \\ \nabla_{\mathbf{x}_k} \xi_{i,k,j} &= 2 |\mathbf{x}_{j+1} - \mathbf{x}_j|^2 (\mathbf{x}_k - \mathbf{x}_i) \\ &\quad - 2 ((\mathbf{x}_{j+1} - \mathbf{x}_j) \cdot (\mathbf{x}_k - \mathbf{x}_i)) (\mathbf{x}_{j+1} - \mathbf{x}_j) \\ \nabla_{\mathbf{x}_k} \eta_{i,k,j} &= \beta |\mathbf{x}_j - \mathbf{x}_{j+1}|^\alpha |\mathbf{x}_k - \mathbf{x}_i|^{\beta-2} (\mathbf{x}_k - \mathbf{x}_i)\end{aligned}$$

With all these cases covered, one may back substitute to (D.1)  $\sim$  (D.4) to acquire the exact gradient by summing over the  $4(N - 3)$  pairs of indices.

## References

- [1] “6. Globally Convergent Modifications of Newton’s Method”. In: *Numerical Methods for Unconstrained Optimization and Nonlinear Equations*, pp. 111–154. DOI: 10.1137/1.9781611971200.ch6. eprint: <https://pubs.siam.org/doi/pdf/10.1137/1.9781611971200.ch6>. URL: <https://pubs.siam.org/abs/10.1137/1.9781611971200.ch6>.
- [2] Amir Beck. “Chapter 8: Primal and Dual Projected Subgradient Methods”. In: *First-Order Methods in Optimization*, pp. 195–245. DOI: 10.1137/1.9781611974997.ch8. eprint: <https://pubs.siam.org/doi/pdf/10.1137/1.9781611974997.ch8>. URL: <https://pubs.siam.org/abs/10.1137/1.9781611974997.ch8>.

- [3] G. D. Bergland. “A guided tour of the fast Fourier transform”. In: *IEEE Spectrum* 6.7 (1969), pp. 41–52. DOI: [10.1109/MSPEC.1969.5213896](https://doi.org/10.1109/MSPEC.1969.5213896).
- [4] Gregory Buck and Jeremy Orloff. “A simple energy function for knots”. In: *Topology and its Applications* 61.3 (Feb. 1995), pp. 205–214. DOI: [10.1016/0166-8641\(94\)00024-w](https://doi.org/10.1016/0166-8641(94)00024-w).
- [5] Eleonora Di Nezza, Giampiero Palatucci, and Enrico Valdinoci. “Hitchhiker’s guide to the fractional Sobolev spaces”. In: *Bulletin des Sciences Mathématiques* 136.5 (2012), pp. 521–573. ISSN: 0007-4497. DOI: <https://doi.org/10.1016/j.bulsci.2011.12.004>. URL: <https://www.sciencedirect.com/science/article/pii/S0007449711001254>.
- [6] Daniel A. Gilchrist. *Histone*. Apr. 2023. URL: <https://www.genome.gov/genetics-glossary/histone>.
- [7] Derek Moulton. *C5.9 Mathematical Mechanical Biology*. Lecture Note. 2022.
- [8] Jim Oliver. *M5 Fourier Series and PDEs*. Lecture Note. 2019.
- [9] Richard Reuter. “Solving (Cyclic) Tridiagonal Systems”. In: *SIGAPL APL Quote Quad* 18.3 (Mar. 1988), pp. 6–12. ISSN: 0163-6006. DOI: [10.1145/44164.44165](https://doi.org/10.1145/44164.44165). URL: <https://doi.org/10.1145/44164.44165>.
- [10] Endre Süli. *B6.1 Numerical Solution of Partial Differential Equations*. Lecture Note. 2021.
- [11] Lloyd N. Trefethen. *Approximation Theory and Approximation Practice*. Extended Edition. Philadelphia, Pa: SIAM, 2020.
- [12] Chris Yu, Henrik Schumacher, and Keenan Crane. “Repulsive Curves”. In: *ACM Transactions on Graphics* 40.2 (Apr. 2021), pp. 1–21. DOI: [10.1145/3439429](https://doi.org/10.1145/3439429).